https://doi.org/10.1016/j.tre.2023.103071

Equilibrium analysis of morning commuting and parking under spatial capacity allocation in the autonomous vehicle environment

Xiang Zhang[a], Wei Liu[b,*], Michael Levin[c], S. Travis Waller[a]

[a] *College of Transportation Engineering, Dalian Maritime University, Dalian, Liaoning, China*

[b] *Department of Aeronautical and Aviation Engineering, The Hong Kong Polytechnic University, Hong Kong, China*

[c] *Department of Civil, Environmental, and Geo-Engineering, University of Minnesota, United States*

[d] *"Friedrich List" Faculty of Transport and Traffic Sciences, Technische Universität Dresden, Germany*

[*] *Corresponding author: Tel.: +852 3400 2386; Email: wei.w.liu@polyu.edu.hk*

Abstract

This study analytically investigates the morning commuting and parking patterns of autonomous vehicles (AVs) under different spatial road capacity allocation schemes (i.e., capacity split between inbound and outbound travel directions). Given that self-driving AV might park far away from commuters' destination, we investigate equilibrium departure/arrival and parking patterns for AVs subject to the spatial road capacity allocation. We also analyse the system optimum traffic pattern for AV morning commute under a given capacity allocation scheme. Furthermore, we examine optimal capacity allocation strategies under user equilibrium and system optimum AV traffic patterns, respectively, which aim to minimise the total system travel cost. Numerical studies are conducted to illustrate the model and analysis. The results reveal the sensitivity of different efficiency metrics with respect to AV parking supply and road capacity allocation schemes, and provide insights into the infrastructure management with future automated transport.

Keywords: autonomous vehicles, morning commute, spatial capacity allocation, bottleneck model, user equilibrium, system optimum

Acknowledgement. We would like to thank the reviewers very much for their useful comments, which helped improve this paper substantially. This study is supported by the National Natural Science Foundation of China (Grant No. 52202380) and the Australian Research Council (Discovery Projects, DP190102873).

Equilibrium analysis of morning commuting and parking under spatial capacity allocation in the autonomous vehicle environment

Abstract

This study analytically investigates the morning commuting and parking patterns of autonomous vehicles (AVs) under different spatial road capacity allocation schemes (i.e., capacity split between inbound and outbound travel directions). Given that self-driving AV might park far away from commuters' destination, we investigate equilibrium departure/arrival and parking patterns for AVs subject to the spatial road capacity allocation. We also analyse the system optimum traffic pattern for AV morning commute under a given capacity allocation scheme. Furthermore, we examine optimal capacity allocation strategies under user equilibrium and system optimum AV traffic patterns, respectively, which aim to minimise the total system travel cost. Numerical studies are conducted to illustrate the model and analysis. The results reveal the sensitivity of different efficiency metrics with respect to AV parking supply and road capacity allocation schemes, and provide insights into the infrastructure management with future automated transport.

Keywords: autonomous vehicles, morning commute, spatial capacity allocation, bottleneck model, user equilibrium, system optimum

1 Backgrounds

With the development of intelligent motion systems and robotics, autonomous vehicles (AVs) are expected to reshape the future transportation, with their functions of adaptive steering control and parking guidance or assistance (Burns, 2013). Given the self-driving capability of AVs, AVs might park far away from commuters' destinations after dropping off the commuters. This new behaviour feature will substantially change the parking and traffic patterns in urban areas (e.g., Liu, 2018; Levin et al., 2020; Zhang et al., 2021). In this context, this study develops road capacity allocation schemes (i.e., capacity allocation between inbound and outbound travel directions) to improve AV traffic efficiency. Specifically, through the capacity allocation scheme, such as contraflow lane reversal, the capacity of congested arterial roads can be temporarily increased. This can potentially help mitigate traffic congestion during peak hours. For example, Fosgerau (2011) proposed a congested bottleneck model under a fast lane scheme wherein capacity is allocated to different classes of travellers, and the results showed that the scheme is welfare improving. Hausknecht et al. (2011) proposed a bi-level model for contraflow lane reversal, and reported that the temporary increase in the service capacity of congested roads can relieve traffic congestion during rush hours and evacuation events. Di and Yang (2020) developed a lane-based optimisation model for the capacity allocation scheme, which aimed to better service the travel demand by appropriately allocating capacity for reversible lanes. However, most previous work proposed the capacity allocation scheme for a non-AV situation, wherein AVs were not taken into consideration and new commuting and parking behaviour of AVs are not considered.

In the non-AV environment, when commuters drive a human-driven vehicle (HV) for work or business in the morning, they need to find a parking space, where the parking space should be located within the acceptable walking distance.[1] Given the potential driving automation, the AV journey could proceed as follows: the AV departs from the origin (of travellers), drops travellers (or passengers) at the destination, and then drives itself to an inexpensive parking space which can be far away from the destination. Such an AV travel process not only makes differences to the parking

[1] In this context, many studies have examined different parking supply and management strategies, e.g., managing cruising for parking (e.g., Arnott and Inci, 2006; Inci and Lindsey, 2015; Liu and Geroliminis, 2016; Li et al., 2020), parking pricing strategies (e.g., Arnott et al., 1991; Qian et al., 2011; Qian et al., 2012; Qian and Rajagopal, 2014; He et al., 2015; Ma and Zhang, 2017; Wang et al., 2019), parking permit or reservation systems (e.g., Zhang et al., 2011; Liu et al., 2014; Chen et al., 2015; Tian et al., 2019), and park-and-ride (Liu et al., 2009; Liu and Geroliminis, 2017).

behaviour, but also could lead to different traffic patterns from that for non-AVs. In particular, in the AV environment, there can be congested bottlenecks both at the inbound (from home to the workplace) and outbound (from the workplace to home/parking) directions during morning peak hours, while quite often only the former might exist in the non-AV environment. The main difference between these two bottlenecks is that the inbound bottleneck is caused by occupied trips (AVs carrying commuters), while the outbound one is caused by empty vehicle trips via AV self-driving for the parking. Also, occupied trips and empty vehicle trips might be valued differently in terms of user cost and social cost, which should be appropriately managed.

Existing studies (e.g., Levin and Boyles, 2015) indeed already showed that AV parking behaviours can have significant impacts on traffic congestion; each traveller generates two AV trips (one to the destination, and one to parking) which increases travel demand. Liu (2018) and Levin et al. (2019) further showed that departure times affected the congestion caused by these empty parking trips. However, most previous work on redesigning road infrastructure for AVs often ignored the changes in trip patterns that result from AV use by travellers.

Given the above AV commuting and parking problem with multiple potential congested locations, this study examines how to optimally allocate road capacity (e.g., inbound and outbound directions) in the morning commute. In the non-AV environment, allocating capacity to inbound arterial roads helps improve the performance for the traffic corridor in most cases, as traffic congestion usually occurs in the inbound direction. By contrast, in the AV environment, such a capacity allocation strategy may deteriorate traffic congestion caused by empty AV trips (heading for parking) in the outbound direction, due to the reduction of the service capacity of the outbound bottleneck. The capacity allocation problem is more complicated for the AV situation than the non-AV one, where there exist complex endogenous interactions among aforementioned (at least) two road bottlenecks. Some relevant studies in the literature investigate a two-tandem bottleneck or serial-bottleneck system (Kuwahara, 1990; Wang et al., 2021). In comparison with previous works, the research problem in this study involves the allocation of the same total service capacity to the two bottlenecks in the opposite directions where trip purposes and cost rates are different.

A few recent studies have derived the AV morning commuting and parking pattern by incorporating the AV travel process into the equilibrium analysis. For example, Liu (2018) proposed the joint equilibrium of departure time and parking location choices for AV morning commutes. That study was then extended by incorporating the AV evening commute (Zhang et al, 2019a) and by considering the AV route choice at the network-wide level (Zhang et al., 2019b, 2021; Levin et al.,

2020). However, none of these studies takes the spatial capacity allocation into consideration, such as dynamic lane reversal, reversible lanes. Appropriate capacity allocation can help alleviate peak hour congestion, while the majority of previous work proposed the capacity allocation scheme for a non-AV environment. Among a few exceptions, Duell et al. (2016) and Levin and Boyles (2016) proposed a traffic assignment problem with dynamic lane reversal for AVs by using the cell transmission model, but the AVs' integrated travel and parking activities via self-driving was not fully considered.

The contributions of this study are focused on addressing two open questions: (i) what are the main features of commuting and parking patterns when spatial road capacity allocation is considered in a fully autonomous environment? (ii) what are the optimal capacity allocation strategies to improve system traffic efficiency with AVs? This study employs a linear city modelling framework, wherein the residential area and the CBD are connected by a traffic corridor (Vickrey, 1969; Arnott et al., 1991; Zhang et al., 2008; Li and Huang, 2017; Tang et al., 2021). The analytically tractable bottleneck model is adopted to capture AV traffic dynamics under different road capacity allocations.[2] As compared to the existing bottleneck model studies with AV trips (e.g., Liu, 2018), this study further considers road capacity allocation for AVs and quantifies the location of the active bottleneck and the level of congestion that are governed by the proposed spatial capacity allocation scheme. Specifically, for AV morning commutes under capacity allocation, traffic congestion could occur at the inbound bottleneck, or outbound bottleneck, or both. Overall, this study provides insights in relation to capacity allocation strategies for future automated transportation systems.

The rest of this paper is organised as follows. Section 2 analyses the morning commute equilibrium considering AV parking under a given capacity allocation scheme. We formulate the analytical model, and derive the AV traffic pattern at equilibrium under different conditions. Section 3 investigates the system optimum AV traffic pattern under a given capacity allocation scheme. Section 4 investigates the optimal capacity allocation strategy under either user equilibrium or system optimum

[2] It is noteworthy that there is a branch of studies examining a linear traffic corridor with multiple origins and/or destinations for AV travel problems (e.g., Wu et al., 2020); road pricing problems (e.g., Lin et al., 2018); bi-modal system design problems (e.g., Li et al., 2012). This paper considers a single origin-destination pair for analytical tractability. Future studies may further incorporate multiple origins and/or destinations.

traffic pattern. Section 5 presents numerical studies. Section 6 concludes this study and discusses future research directions.

2 User Equilibrium under Capacity Allocation in Fully Autonomous Environment

2.1 Travel disutility of AVs with capacity allocation

In this section, we present the equilibrium analysis on the morning commute with autonomous vehicles considering different capacity allocations. We investigate the joint equilibrium in terms of departure time from home and parking location choice, where the former and the latter are intercorrelated for AV morning commutes. We consider a linear city network for AV morning commute under a given capacity allocation scheme (capacity split between the inbound and outbound directions), which is depicted in Figure 1.

As shown in Figure 1, to complete the journey in the morning, AVs need to pass through two bottlenecks along the corridor, at which traffic congestion occurs. One bottleneck is named as "inbound bottleneck", which is located on the way from the residential area to the workplace; the other one is named as "outbound bottleneck", which is located on the way from the workplace to the parking area. We investigate the scenario wherein the capacity allocation scheme is to be considered. Note that in this context, we investigate a situation where there exist multiple lanes in each direction. Initially, the total capacity of the traffic corridor is set as $2s$, while the service capacity for each of the inbound and outbound directions is assumed to be s. We assume that the total capacity is conserved, which remains as $2s$. For the capacity allocation scheme, the capacity of τ is transferred from the outbound direction to the inbound direction for the morning commute with AVs. For analytical tractability, τ is assumed to be a continuous variable, which ranges from zero to the one-way service capacity s. As a result, the capacity of the inbound bottleneck is adjusted to be $(s+\tau)$, while that of the outbound bottleneck becomes $(s-\tau)$. For capacity allocation, another option is that we reduce the capacity of the inbound bottleneck but enhance the capacity of the outbound one for the morning commute. Given that the arrival rate to the outbound bottleneck cannot be greater than the service capacity of the inbound bottleneck, the capacity transferred to the outbound direction would be wasted under this option. In the meantime, the reduced service capacity for the inbound direction could worsen the traffic performance. Hence, in this study, we only consider the capacity allocation strategy that leads to the potential expansion of inbound capacity along with the reduction of outbound capacity for AV morning commute.

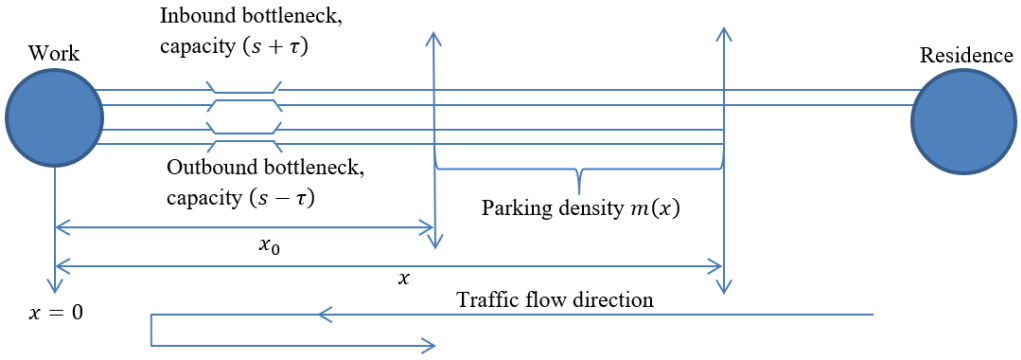

Figure 1. The linear city network under a given capacity allocation

As depicted in Figure 1, the travelling process of AV morning commutes under the proposed capacity allocation scheme follows the procedure: Depart from home → Pass the inbound bottleneck → Reach the workplace and drop off commuters → Pass the outbound bottleneck (AV self-driving) → Find an appropriate parking space (AV self-driving). The outbound bottleneck is located between the workplace and the closest parking space where $x = x_0$. Note that to allow analytical derivations, we assume a constant parking density (along the way of AVs' self-driving parking trip), i.e. $m(x) = m,\ x \geq x_0$. Note that we do not consider parking within a walking distance to the final destination and the walking process in this study.

The setting in Figure 1 has distinctive characteristics with regards to the two-bottleneck system in the non-AV situation (Kuwahara, 1990; Qian et al., 2012). In this study, all AVs must pass the two bottlenecks as shown in Figure 1 in the morning commutes, where the total capacity of the two bottlenecks are given while the capacity split between the two bottlenecks can be optimized. Moreover, the inbound and outbound bottlenecks are associated with occupied-AV trips and empty-AV trips, respectively. Consequently, the cost rates of traversing the two bottlenecks are not identical, which is considered by AV commuters when making the choice of departure time from home. This could then affect the equilibrium traffic pattern and lead to multiple scenarios, which differ from those in the existing literature on non-AV commutes (Wang et al., 2021; Wei et al., 2022).

For the above AV travel process, it is noteworthy that AV commuters experience the congestion at the inbound bottleneck during the occupied AV trip, while the congestion at the outbound bottleneck is experienced by the empty AV trip. With the introduced capacity allocation plan, the departure rate from the workplace after dropping off commuters can be as high as the capacity of the inbound capacity, i.e.

$(s+\tau)$. This means that the arrival rate to the outbound bottleneck can be larger than the service capacity of the outbound capacity, i.e. $(s-\tau)$. Hence, the congestion could occur both at the inbound bottleneck and at the outbound bottleneck. This is different from the existing literature on AV equilibrium analysis without consideration of the capacity allocation scheme, in which the outbound bottleneck is never active in the morning commute (Liu, 2018; Zhang et al., 2019a).

Before we formulate the travel disutility under capacity allocation for AV commutes, several assumptions on travel behaviour and parking are summarised below (please refer to Appendix A for mathematical notations):

(i) Commuters are homogeneous, and they: a) have the same official work start time; b) alight at the workplace and let AVs cruise for parking spots via self-driving.

(ii) The cost rate λ (cost per unit driving time) for AV self-driving is assumed to be independent of the travel speed.

(iii) The cost rates (costs or schedule penalties per unit time) satisfy the conditions: a) $\alpha > \lambda > 0$; b) $\gamma > \alpha > \beta > 0$, which are consistent with the empirical evidence (Soteropoulos et al., 2019).

(iv) The cost for free-flow travel between the residential area and the workplace and the cost for traversing the road segment between $x = 0$ and $x = x_0$ without queuing delay are assumed to be zero, as they are the same to all AV commuters and do not affect the analysis.

Based on the allocation of service capacity, the travel disutility for AV commuters who departs at time t and parking at location x can be formulated as follows. The mathematical notations used throughout this paper are listed in Appendix A, unless otherwise defined.

$$c(t,x) = \alpha \cdot T_1(t) + \beta \cdot [t^* - t - T_1(t)]^+ + \gamma \cdot [t + T_1(t) - t^*]^+ + \lambda w x(t) + \lambda \cdot T_2(t), \quad (1)$$

where $[\cdot]^+ \equiv max\{\cdot, 0\}$. $T_1(t)$ and $T_2(t)$ are respectively the queuing delay experienced at the inbound bottleneck and at the outbound bottleneck by the commuters departing at time t in the morning. The first term is the travel cost for queuing delay at the inbound bottleneck; the second term is the penalty cost for early arrival; the third term is the penalty cost for late arrival; the fourth term is the cost of driving to an appropriate parking space via AV self-driving (free-flow time to the parking) where w is the travel time needed to cover a unit distance by AV self-driving; the fifth term is the cost for queuing delay at the outbound bottleneck during searching-for-parking

activity. Note that the parking location x is dependent on the departure time t, i.e., $x = x(t)$, given that the travellers who depart earlier have the priority to choose the preferred parking location. The constant free-flow travel time cost for the inbound trip is assumed as zero. The constant free-flow travel time cost for the outbound trip from the workplace to the location x_0 is also assumed as zero. These two constant costs are the same to all AV commuters and will not affect the analysis. Also, in Eq. (1), it is assumed that no toll and no parking fee is charged regardless of time and location, so we indeed investigate the no-toll and no-fee traffic equilibrium for AVs in this context.

At user equilibrium, AVs commuters would always choose to park at the closest space available, in order to reduce the travel cost for AV self-driving. In this study, we consider sufficient AV parking supply, which allows later arrivals to park far away from the workplace under the introduced parking distribution. Given this, the following relationship holds

$$\int_{t_s}^{t} f(v)dv = \int_{x_0}^{x(t)} m(u)du \;\Rightarrow\; f(t) = m(x) \cdot \frac{dx(t)}{dt}. \tag{2}$$

f is the time-dependent departure rate from home. t_s is the departure time of the first AV commuter in the morning. x_0 indicates the location of the closest parking space to the workplace, so we have $\int_0^{x_0} m(u)du = 0$. Under the assumption of the constant AV parking density, i.e., $m(x) = m$, we have

$$\frac{dx(t)}{dt} = \frac{f(t)}{m}. \tag{3}$$

In addition, we assume $\beta > \frac{\lambda ws}{m}$ in this study (Arnott et al., 1991; Liu, 2018; Zhang et al., 2019a). This means that, when capacity allocation is not taken into consideration, the marginal saving in the schedule delay cost by postponing a unit departure time for early arrivals is higher than the marginal increase in the cost of AV self-driving for the parking purpose. This ensures that the service capacity is made full use of wherein traffic congestion occurs at the inbound bottleneck, when capacity allocation is not deployed at the initial stage, i.e., $\tau = 0$ and the inbound and outbound bottlenecks have the same capacity. However, when capacity allocation strategy is implemented, two possible scenarios have to be considered. Scenario 1 is when the traffic congestion occurs at both bottlenecks, while Scenario 2 is when the traffic congestion occurs at the outbound bottleneck only. These two scenarios will be

analysed in the following subsections. Note that under the assumption $\beta > \frac{\lambda w s}{m}$, congestion (or queuing) always occurs at the outbound bottleneck.

With the introduced travel disutility, we can define the joint user equilibrium of departure time and parking location for AV commutes under capacity allocation as follows: Every AV commuter seeks to minimise their individual travel disutility, which is formulated as $c(t,x)$ in Eq. (1); As a result, all commuters have the same travel disutility regardless of departure time and parking location choices, and no one can further reduce their own travel cost by unilaterally changing their own travel strategies when the user equilibrium is reached.

With the above setting in mind, we are now ready to investigate the equilibrium travel and parking pattern with AVs in the morning commute when spatial capacity allocation is implemented. We can categorise all the possible scenarios into two groups, depending on where traffic congestion could occur. If the departure rate from home is no greater than the service capacity of the outbound bottleneck, i.e., $(s-\tau)$, it simply means a capacity waste where none of the bottlenecks is active. We do not include this scenario in our presented analysis, as it does not require capacity adjustment. Hence, in our modelling framework, we consider an active outbound bottleneck, and have: (i) Scenario 1, where congestion occurs at both bottlenecks, and (ii) Scenario 2, where congestion occurs at the outbound bottleneck only. We will discuss the equilibrium AV traffic pattern under each scenario in the following subsections.

2.2 Scenario 1

In Scenario 1, given that traffic congestion occurs at both bottlenecks, we have:

$$f_e > s + \tau, \tag{4}$$

where f_e represents the departure rate for early arrival. To ensure that Eq. (4) holds, the following condition must be satisfied:

$$\beta > \lambda \frac{w(s+\tau)}{m} + \lambda \frac{2\tau}{s-\tau}. \tag{5}$$

The physical meaning of the above condition is that, under a given capacity allocation, the marginal saving in the early schedule delay cost by postponing a unit of time is greater than the marginal increase in the cost of AV self-driving for cruising for a parking space including the cost of queuing delay, with traffic congestion experienced at both bottlenecks.

In Scenario 1, to calculate the queuing delay time, we have, for the inbound bottleneck,

$$T_1(t) = \frac{q_1(t)}{s+\tau};\ q_1(t) = \int_{t_s}^{t} f(v)dv - (s+\tau)(t-t_s), \tag{6}$$

where $q_1(t)$ is the queue length at the inbound bottleneck for commuters departing at time t; and for the outbound bottleneck,

$$T_2(t) = \left[\frac{\int_{t_s}^{t}(f(v)-(s-\tau))dv}{s-\tau}\right] - \left[\frac{\int_{t_s}^{t}(f(v)-(s+\tau))dv}{s+\tau}\right] = \frac{2\tau}{s^2-\tau^2}\cdot\int_{t_s}^{t} f(v)dv, \tag{7}$$

where the term $\left[\frac{\int_{t_s}^{t}(f(v)-(s-\tau))dv}{s-\tau}\right]$ represents the total queuing delay at the inbound and outbound bottlenecks, experienced by commuters departing at time t in Scenario 1; the term $\left[\frac{\int_{t_s}^{t}(f(v)-(s+\tau))dv}{s+\tau}\right]$ represents the queuing delay at the inbound bottleneck.

To obtain the equilibrium commuting pattern for AVs, we take the first-order derivatives of the travel disutility $c(t,x)$ with regards to the departure time t, substituting Eqs. (3), (6) and (7), and derive the following equations:

For early arrival,

$$\frac{dc(t,x)}{dt} = \alpha\cdot\frac{f(t)-(s+\tau)}{s+\tau} - \beta\cdot\frac{f(t)}{s+\tau} + \lambda\cdot w\frac{f(t)}{m} + \lambda\cdot\frac{2\tau}{s^2-\tau^2}f(t). \tag{8}$$

For late arrival,

$$\frac{dc(t,x)}{dt} = \alpha\cdot\frac{f(t)-(s+\tau)}{s+\tau} + \gamma\cdot\frac{f(t)}{s+\tau} + \lambda\cdot w\frac{f(t)}{m} + \lambda\cdot\frac{2\tau}{s^2-\tau^2}f(t). \tag{9}$$

Given that each AV commuter should have the identical travel disutility at equilibrium, the relationship $\frac{dc(t)}{dt} = 0,\ t\in[t_s,t_e]$ holds. Hence, for early arrival, we can obtain the departure rate f_e as follows

$$f_e = \frac{\alpha}{\left(\alpha-\beta+\frac{\lambda w(s+\tau)}{m}+\lambda\cdot\frac{2\tau}{s-\tau}\right)}(s+\tau). \tag{10}$$

For late arrival, we can obtain the departure rate f_l as follows

$$f_l = \frac{\alpha}{\left(\alpha+\gamma+\frac{\lambda w(s+\tau)}{m}+\lambda\cdot\frac{2\tau}{s-\tau}\right)}(s+\tau). \tag{11}$$

It can be seen that the relationship $f_e > s+\tau$ must hold under the condition $\beta > \lambda\frac{w(s+\tau)}{m} + \lambda\frac{2\tau}{s-\tau}$ (Eq. (5)).

Based on the above analysis, the equilibrium AV commuting pattern for Scenario 1 can be depicted as Figure 2. The green curve PRY represents the cumulative departure from home, i.e. the cumulative arrival at the inbound bottleneck; the red curve PY represents the cumulative flow arriving at the workplace, which is equal to the cumulative departure from the inbound bottleneck, as well as the cumulative arrival to the outbound bottleneck; the blue curve PW represents the cumulative departure from the outbound bottleneck; the purple curve PV represents the cumulative arrival at the parking place.

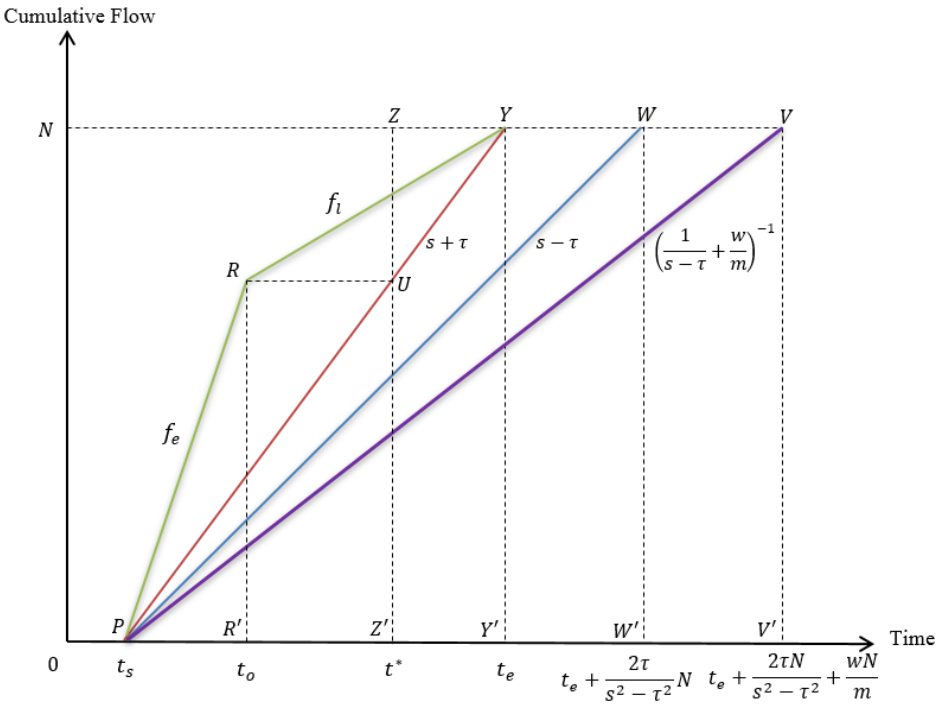

Figure 2. AV traffic pattern for morning commute at user equilibrium in Scenario 1

Let t_s and t_e be the departure time for the first commuter and the last commuter, respectively. These times are derived by studying the equilibrium behaviour. The flow conservation constraint can be written as follows

$$(t_e - t_s) \cdot (s + \tau) = N. \tag{12}$$

At equilibrium, the travel disutility for the first commuter is equal to that for the last commuter. Hence, we have

$$\beta \cdot (t^* - t_s) = \gamma \cdot (t_e - t^*) + \lambda \cdot w\frac{N}{m} + \lambda \cdot T_2(t_e). \tag{13}$$

Based on Figure 2, $T_2(t_e)$ can be calculated as follows

$$T_2(t_e) = \frac{N}{s-\tau} - \frac{N}{s+\tau} = \frac{2\tau}{s^2-\tau^2}N. \tag{14}$$

Combining Eqs. (12) (13) and (14), we can get the departure time for the first and the last commuters:

$$\begin{aligned} t_s &= t^* - \frac{N}{\beta+\gamma}\left(\frac{\lambda w}{m} + \frac{2\lambda\tau}{s^2-\tau^2} + \frac{\gamma}{s+\tau}\right); \\ t_e &= t^* + \frac{N}{\beta+\gamma}\left(\frac{\beta}{s+\tau} - \frac{\lambda w}{m} - \frac{2\lambda\tau}{s^2-\tau^2}\right). \end{aligned} \tag{15}$$

Furthermore, based on Figure 2, the departure time corresponding to the on-time arrival, denoted as t_o, can be calculated as follows

$$t_o = t^* - \frac{N}{\beta+\gamma}\left(\frac{\lambda w}{m} + \frac{2\lambda\tau}{s^2-\tau^2} + \frac{\gamma}{s+\tau}\right)\left(\frac{\beta - \frac{\lambda w(s+\tau)}{m} - \lambda\cdot\frac{2\tau}{s-\tau}}{\alpha}\right). \tag{16}$$

In addition, the total numbers of early arrival and late arrival, N_e and N_l, which equals $(t_o - t_s)f_e$ and $(t_e - t_o)f_l$, are respectively

$$\begin{aligned} N_e &= \frac{s+\tau}{\beta+\gamma}\left(\frac{\lambda w}{m} + \frac{2\lambda\tau}{s^2-\tau^2} + \frac{\gamma}{s+\tau}\right)N; \\ N_l &= \frac{s+\tau}{\beta+\gamma}\left(\frac{\beta}{s+\tau} - \frac{\lambda w}{m} - \frac{2\lambda\tau}{s^2-\tau^2}\right)N. \end{aligned} \tag{17}$$

Note that, under the assumption $\beta > \lambda\frac{w(s+\tau)}{m} + \lambda\frac{2\tau}{s-\tau}$, the relationship $0 < N_e, N_l < N$ holds in all cases. To investigate how N_e and N_l vary with capacity allocation, we check the first-order derivatives of N_e and N_l with respect to τ,

$$\frac{dN_e}{d\tau} = \frac{s+\tau}{\beta+\gamma}\left[\frac{\lambda w}{m(s+\tau)} + \frac{2\lambda\left((\tau^2+s^2)+\tau(s-\tau)\right)}{(s^2-\tau^2)^2}\right];$$
$$\frac{dN_l}{d\tau} = -\frac{s+\tau}{\beta+\gamma}\left[\frac{\lambda w}{m(s+\tau)} + \frac{2\lambda\left((\tau^2+s^2)+\tau(s-\tau)\right)}{(s^2-\tau^2)^2}\right]. \quad (18)$$

One can readily verify that $\frac{dN_e}{d\tau} > 0$ and $\frac{dN_l}{d\tau} < 0$. This means that when the capacity allocation scheme is implemented, the total number of early arrivals is monotonically increasing with the increase in the transferred capacity τ from outbound road to inbound road, while in the meantime, the total number of late arrivals is decreasing. There are two main reasons. First, when we increase the service capacity of the inbound bottleneck, the queue length will be shortened, which leads to a lower queuing delay cost. Given this, more commuters are encouraged to depart from home early. Second, when the transferred capacity increases, the service capacity of the outbound bottleneck becomes lower, resulting in more congested flow during the cruising-for-parking activity via AV self-driving. This means that the queuing delay cost at the outbound bottleneck would go up, which incentivises more AVs to depart from home early to avoid the potential high cost of AV self-driving under severe traffic congestion after dropping off commuters at their workplace.

Based on the derived AV commuting pattern for Scenario 1, the total system travel cost at user equilibrium ($TSTC_{UE}$) can be calculated as follows

$$TSTC_{UE} = TSTC_{UE,1} = \left[\frac{\beta N}{\beta+\gamma}\left(\frac{\lambda w}{m} + \frac{2\lambda\tau}{s^2-\tau^2} + \frac{\gamma}{s+\tau}\right)\right]N. \quad (19)$$

where the term in the square bracket is the individual travel disutility at equilibrium. We can also evaluate several system efficiency metrics for the AV commute at user equilibrium. Here, we denote the area of the polygon Ω as A_Ω, wherein Ω is described by specifying node labels in Figure 2. The total cost of queuing delay experienced at the inbound bottleneck, denoted as TQ_1, is

$$TQ_1 = \alpha \cdot A_{PRY} = 0.5 \cdot \frac{1}{\beta+\gamma}\left(\frac{\lambda w}{m} + \frac{2\lambda\tau}{s^2-\tau^2} + \frac{\gamma}{s+\tau}\right)\left(\beta - \frac{\lambda w(s+\tau)}{m} - \lambda \cdot \frac{2\tau}{s-\tau}\right)N^2. \quad (20)$$

The total cost of queuing delay experienced by empty vehicles at the outbound bottleneck during AV self-driving, denoted as TQ_2, is

$$TQ_2 = \lambda \cdot A_{PYW} = 0.5\lambda\left(\frac{2\tau}{s^2-\tau^2}\right)N^2. \quad (21)$$

The total cost of schedule delay for early arrival, denoted as TS_e, is

$$TS_e = \beta \cdot A_{UPZ'} = 0.5\beta \frac{s+\tau}{(\beta+\gamma)^2} \left(\frac{\lambda w}{m} + \frac{2\lambda\tau}{s^2-\tau^2} + \frac{\gamma}{s+\tau}\right)^2 N^2. \quad (22)$$

The total cost of schedule delay for late arrival, denoted as TS_l, is

$$TS_l = \gamma \cdot A_{UZY} = 0.5\gamma \frac{s+\tau}{(\beta+\gamma)^2} \left(\frac{\beta}{s+\tau} - \frac{\lambda w}{m} - \frac{2\lambda\tau}{s^2-\tau^2}\right)^2 N^2. \quad (23)$$

The total cost of schedule delay, denoted as TS, is

$$TS = TS_e + TS_l = 0.5 \frac{(s+\tau)N^2}{(\beta+\gamma)^2} \left[\beta \left(\frac{\lambda w}{m} + \frac{2\lambda\tau}{s^2-\tau^2} + \frac{\gamma}{s+\tau}\right)^2 + \gamma \left(\frac{\beta}{s+\tau} - \frac{\lambda w}{m} - \frac{2\lambda\tau}{s^2-\tau^2}\right)^2\right]. \quad (24)$$

The total cost for cruising-for-parking via AV self-driving without traffic congestion is

$$TP = \lambda \cdot A_{PWV} = 0.5 \frac{\lambda w}{m} N^2. \quad (25)$$

The total AV self-driving cost is

$$TSD = TQ_2 + TP = 0.5\lambda \left(\frac{2\tau}{s^2-\tau^2} + \frac{w}{m}\right) N^2. \quad (26)$$

Note that when λ approaches zero and m approaches infinity, the equilibrium traffic pattern is formed with the departure times being $t_s = t^* - \frac{\gamma}{\beta+\gamma}\left(\frac{N}{s+\tau}\right)$, $t_e = t^* + \frac{\beta}{\beta+\gamma}\left(\frac{N}{s+\tau}\right)$ and the departure rates being $f_e = \frac{\alpha}{(\alpha-\beta)}(s+\tau)$, $f_l = \frac{\alpha}{(\alpha+\gamma)}(s+\tau)$. This matches the classic bottleneck model for non-AVs without consideration of walking (Arnott, 1991). This is because when $\lambda \to 0$, the cost for the process under AV self-driving has been omitted. Then, the queuing delay at the outbound bottleneck caused by the capacity allocation would not incur any travel disutility given that the trip for parking is completed when the AV drives itself after dropping commuters. With the assumption $m \to \infty$ added, no one is incentivised to depart earlier for an advantageous parking location to reduce the cost for cruising-for-parking via AV-self driving. Hence, the situation is equivalent to that under the classic bottleneck setting wherein the inbound bottleneck capacity is increased from s to $s+\tau$.

2.3 Scenario 2

In this scenario, the traffic congestion occurs at the outbound bottleneck only, where the following condition holds:

$$\lambda\frac{w(s-\tau)}{m} < \beta \le \lambda\frac{w(s+\tau)}{m} + \lambda\frac{2\tau}{s-\tau}. \quad (27)$$

$\beta > \lambda\frac{w(s-\tau)}{m}$ ensures that traffic congestion occurs at the outbound bottleneck. Note that under the assumption $\beta > \lambda\frac{ws}{m}$, the condition $\beta > \lambda\frac{w(s-\tau)}{m}$ must hold. In Scenario 2, we have Proposition 2.1. For the proof, please refer to Appendix B.

Proposition 2.1. For Scenario 2 where only the outbound bottleneck is active under the capacity allocation scheme, no one would arrive at the workplace later than the official work start time t^* at user equilibrium.

As per Proposition 2.1., every AV commuter arrives at the workplace earlier than t^* or on time in Scenario 2, and we have

$$s - \tau < f_e \le s + \tau;\ f_l = 0. \quad (28)$$

The individual travel disutility for AV commuters in Scenario 2 can be written as follows

$$c(t,x) = \beta \cdot (t^* - t) + \lambda w x(t) + \lambda \cdot T_2(t). \quad (29)$$

In Scenario 2, we have $T_2(t) = \frac{q_2(t)}{s-\tau}$, where $q_2(t)$ is the queue length at the outbound bottleneck during AV self-driving. Given that there is no late arrival in Scenario 2, we have $q_2(t) = \int_{t_s}^{t}\big(f_e(v) - (s-\tau)\big)dv$. By taking the first-order derivative of $c(t)$ with respect to the departure time t, we have

$$\frac{dc(t,x)}{dt} = -\beta + \lambda w\frac{f_e}{m} + \lambda\left(\frac{f_e}{s-\tau} - 1\right). \quad (30)$$

Under the user equilibrium condition, AV commuters have the identical individual travel disutility regardless of the time of departure from home, so $\frac{dc(t,x)}{dt} = 0$ must hold. We then have

$$f_e = \frac{\beta+\lambda}{\lambda\left(\frac{w}{m}+\frac{1}{s-\tau}\right)};\ f_l = 0. \quad (31)$$

It can be easily verified that under the condition described in Eq. (27), the departure rate calculated by using Eq. (31) matches the range indicated by Eq. (28).

Based on the above analysis, the user-equilibrium AV commuting pattern for Scenario 2 can be depicted as Figure 3. The green curve PZ represents the cumulative departure from home (i.e. the cumulative arrival at the inbound bottleneck) as well as

the cumulative arrival at the workplace and the outbound bottleneck; the blue curve PW represents the cumulative departure from the outbound bottleneck; the purple curve PV represents the cumulative arrival at the parking place.

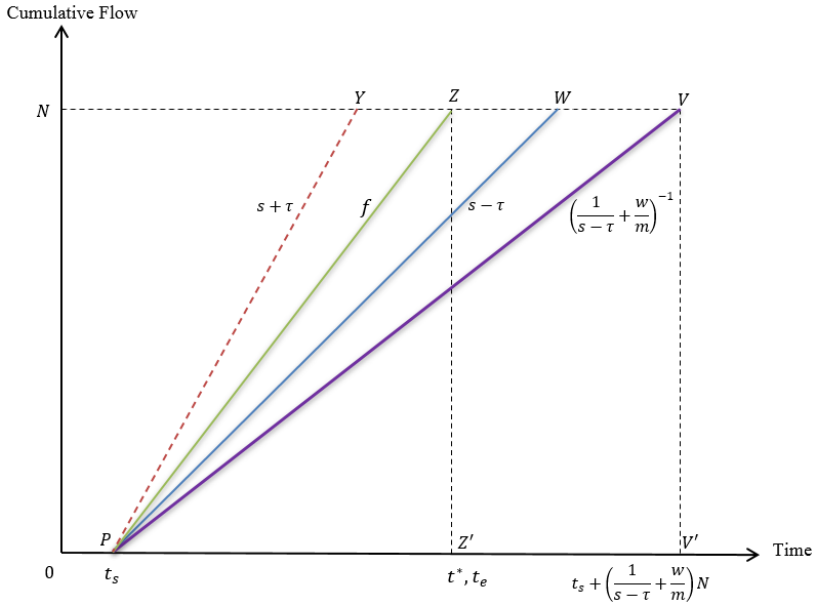

Figure 3. AV traffic pattern for morning commute at user equilibrium in Scenario 2

From Figure 3, we have t_s and t_e in Scenario 2 as follows

$$t_s = t^* - \frac{\lambda\left(\frac{w}{m}+\frac{1}{s-\tau}\right)N}{\beta+\lambda};\ t_e = t^*. \tag{32}$$

The departure time corresponding to the on-time arrival is

$$t_o = t^*. \tag{33}$$

We have $N_e = N$ and $N_l = 0$ in Scenario 2, which are different from those in Scenario 1.

Based on the analysed AV commuting pattern, we can get the total system travel cost in Scenario 2 as follows

$$TSTC_{UE} = TSTC_{UE,2} = \left[\frac{\beta\lambda\left(\frac{w}{m}+\frac{1}{s-\tau}\right)N}{\beta+\lambda}\right]N. \tag{34}$$

where the term in the square bracket is the equilibrium individual travel disutility in Scenario 2.

The aggregate efficiency metrics for Scenario 2 can also be determined. The queuing delay costs are

$$TQ_1 = 0;\ TQ_2 = \lambda \cdot A_{PZW} = 0.5 \cdot \frac{\lambda}{\beta+\lambda}\left(\frac{\beta}{s-\tau} - \frac{\lambda w}{m}\right) N^2. \tag{35}$$

The schedule delay costs are

$$\begin{aligned} &TS_e = \beta \cdot A_{PZZ'} = 0.5 \cdot \frac{\beta\lambda\left(\frac{w}{m}+\frac{1}{s-\tau}\right)}{\beta+\lambda} N^2;\ TS_l = 0; \\ &TS = TS_e + TS_l = 0.5 \cdot \frac{\beta\lambda\left(\frac{w}{m}+\frac{1}{s-\tau}\right)}{\beta+\lambda} N^2. \end{aligned} \tag{36}$$

The total cost for cruising-for-parking via AV self-driving under free flow traffic is

$$TP = \lambda \cdot A_{PWV} = 0.5\frac{\lambda w}{m} N^2. \tag{37}$$

The total AV self-driving cost is

$$TSD = TQ_2 + TP = TSD = TQ_2 + TP = 0.5\frac{\beta}{\beta+\lambda}\left(\frac{\lambda}{s-\tau} + \frac{\lambda w}{m}\right) N^2. \tag{38}$$

It can be verified that at the transition point (i.e. $\beta = \lambda\frac{w(s+\tau)}{m} + \lambda\frac{2\tau}{s-\tau}$) between Scenario 1 and Scenario 2, we have $TSTC_{UE,1} = TSTC_{UE,2} = \left[\frac{\lambda\left(\frac{w(s+\tau)}{m}+\frac{2\tau}{s-\tau}\right)\left(\frac{w}{m}+\frac{1}{s-\tau}\right)}{1+\frac{w(s+\tau)}{m}+\frac{2\tau}{s-\tau}} N\right] N$, where the term in the square bracket is the equilibrium individual travel disutility.

3 System Optimum under a Given Capacity Allocation Scheme

In this section, we investigate the conditions of system optimum (SO) for AV morning commutes under a given capacity allocation scheme, and derive the corresponding traffic pattern. Conceptually, the SO traffic pattern results in the minimum total system travel cost, which excludes any toll or parking fee. In the context of capacity allocation, the following SO conditions should be satisfied: (i) the queuing delay at the inbound bottleneck should be completely eliminated, i.e. $TQ_{1,SO} = 0$; (ii) the sum of the queuing delay cost at the outbound bottleneck and the schedule delay cost should be minimised; (iii) the total free-flow travel cost of AV-self driving for the cruising-for-

parking purpose should be minimised. To meet the above conditions, we have the following constraint for the departure rate f: $f \in [s-\tau, s+\tau]$. This is explained as follows. First, if at any time, $f(t)$ is greater than $(s+\tau)$, it will cause the queuing delay at the inbound bottleneck, which contradicts the SO condition. Second, if $f(t)$ is lower than the service capacity of the outbound bottleneck $(s-\tau)$, it will cause a capacity waste.

For the SO traffic pattern under capacity allocation, we have Proposition 3.1. For the proof, please refer to Appendix B.

Proposition 3.1. At system optimum, the AV traffic pattern for morning commute under capacity allocation is formed in the manner as shown in Figure 4 (the physical meaning of each curve is the same as that for Figure 3), where we have $f_{e,1} = s-\tau$, $f_{e,2} = s+\tau$, $f_l = s+\tau$; $N_e = \frac{\gamma N}{\beta+\gamma}$, $N_l = \frac{\beta N}{\beta+\gamma}$; and, $t_{s,SO} = t^* - \frac{2\lambda\tau}{(\lambda+\beta)(s^2-\tau^2)}N - \frac{\gamma}{(\beta+\gamma)(s+\tau)}N$, $\bar{t} = t^* - \left(\frac{1}{\beta+\lambda} - \frac{1}{\beta+\gamma}\right)\frac{\beta}{(s+\tau)}N$, $t_{e,SO} = t^* + \frac{\beta}{(\beta+\gamma)(s+\tau)}N$.

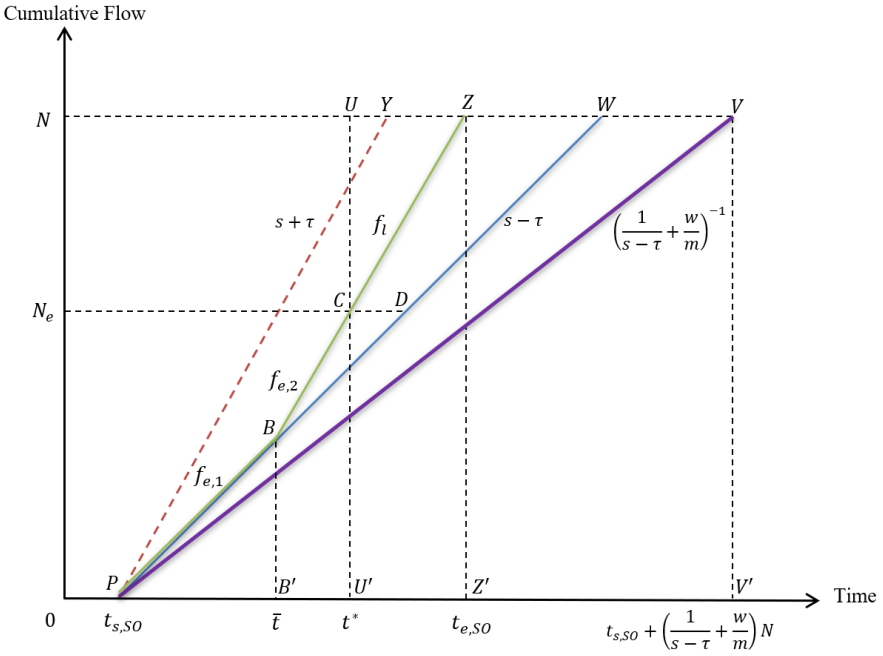

Figure 4. The AV traffic pattern for morning commute at system optimum

Based on Proposition 3.1., when $\tau = 0$, we have $t_{s,SO} = t^* - \frac{\gamma}{(\beta+\gamma)s}N$, $t_{e,SO} = t^* + \frac{\beta}{(\beta+\gamma)s}N$, with the constant flow rate, i.e. $f_{e,1} = f_{e,2} = f_l = s$, at system optimum. This is consistent with the results in the previous study where no capacity allocation scheme is implemented (Liu, 2018). However, when the capacity allocation

scheme is implemented for AV morning commutes, the departure rates cannot be the same for early and late arrivals, which is more complicated than the previous study. This is primarily because the optimal departure rate has to balance the schedule delay cost and the queuing delay cost at the outbound bottleneck under capacity allocation, while the schedule delay cost behaves differently before and after t^*. With $\tau \in (0, s)$, the departure rate from home for late arrival equals $(s + \tau)$. This is because at the time t^*, the queuing delay for the on-time arrival has been already determined, whatever the traffic pattern for early arrival is. Consequently, the time between the official work time t^* and the time of departing the outbound bottleneck for late-arrival trips has been given under the condition $f_l \in [s - \tau, s + \tau]$, as depicted in Figure 4. This time interval consists of two components, i.e. the schedule delay for late arrival and the queuing delay during the AV self-driving activity at the outbound bottleneck. Given that the former is more costly than the latter, f_l should reach its maximum value, i.e., $s + \tau$, in order to lower the schedule delay cost as well as the total travel cost.

In contrast to late arrival, the departure rate from home for early arrival is neither of the two extreme cases where $f_e = s - \tau$ and where $f_e = s + \tau$. This is explained as follows. When $f_e = s - \tau$, the queuing delay at the outbound bottleneck for early arrival can be eliminated. However, the schedule delay for early arrivals will reaches its maximum under this circumstance, while the schedule delay cost rate for early arrival is larger than that for the queuing delay during the AV self-driving activity. When $f_e = s + \tau$, the schedule delay cost for early arrival is reduced, while this would cause two side effects. First, the queuing delay at the outbound bottleneck for early arrival will stem from this situation and reaches its maximum under the condition $f_l \in [s - \tau, s + \tau]$. Second, the queuing delay at the outbound bottleneck for late arrival will be expanded, given that such delay for on-time arrival at time t^* is increased in this situation. Hence, to balance these queuing delays and the schedule delay, the departure behaviour at SO lies between the above-referenced two extreme cases. Mathematically, we can also prove that neither of the two extreme cases satisfies the SO conditions for AV commutes under capacity allocation (please refer to Appendix B for details).

With the derived SO traffic pattern, the total system travel cost at SO can be obtained as follows:

$$TSTC_{SO} = \beta \cdot \left[0.5 \cdot \frac{\lambda^2}{(\lambda+\beta)^2(s-\tau)} N^2 + 0.5 \cdot \frac{(\gamma-\lambda)\beta}{(\lambda+\beta)(\beta+\gamma)(s+\tau)} \left(\frac{\lambda}{\lambda+\beta} + \frac{\gamma}{\beta+\gamma}\right) N^2\right] + \gamma \cdot \left[0.5 \cdot \left(\frac{\beta}{\beta+\gamma}\right)^2 \frac{1}{s+\tau} N^2\right] + \lambda \cdot \left[0.5 \cdot \left(\frac{\beta}{\lambda+\beta}\right)^2 \left(\frac{2\tau}{s^2-\tau^2}\right) N^2\right] + \lambda \cdot \left[0.5 \frac{w}{m} N^2\right]. \quad (39)$$

where the first term and the second one in the right-hand side represent the total schedule delay cost for early arrivals and that for late arrivals, respectively; the third term represents the total queuing delay cost at the outbound bottleneck; the fourth term represents the total cost for cruising-for-parking by AV self-driving under the free-flow condition.

Based on the above, we then have Proposition 3.2.

Proposition 3.2. For the relative system efficiency metric σ, we have:

(i) when $\beta > \lambda\frac{w(s+\tau)}{m} + \lambda\frac{2\tau}{s-\tau}$, σ is equal to $\frac{TSTC_{SO}}{TSTC_{UE,1}}$;

(ii) when $\lambda\frac{w(s-\tau)}{m} < \beta \leq \lambda\frac{w(s+\tau)}{m} + \lambda\frac{2\tau}{s-\tau}$, σ is equal to $\frac{TSTC_{SO}}{TSTC_{UE,2}}$.

Note that, for Proposition 3.2, the value of σ ranges between zero and one, given that the SO traffic pattern is formed in the way that the total system travel cost is minimised. A larger σ reveals that the relative efficiency gain from system optimum against the user equilibrium is less significant.

To eliminate the efficiency loss under user equilibrium with regards to the system optimum, we can impose the time-varying tolling (regime z_1) or location-dependent parking pricing (regime z_2). In other words, under certain regimes, the AV commute pattern under UE can be formed in the SO manner. For details, please refer to Appendix C.

4 Optimal Capacity Allocation

In previous sections, it has already been shown that the capacity allocation scheme can affect AV commuting patterns, both under user equilibrium and system optimum traffic conditions. This section will optimise the capacity allocation for AV morning commute. The motivation is to provide the optimal capacity allocation strategy which minimises the system-level travel cost. As will be shown later, the optimal capacity scheme cannot be determined in a straightforward manner, and it varies with different conditions. In particular, Section 4.1 and Section 4.2 investigate the optimal capacity allocation scheme for AV morning commute under the user equilibrium and system optimum traffic patterns, respectively.

4.1 Optimal capacity allocation under user equilibrium

We now investigate the optimal strategy for capacity allocation for AV morning commutes under user equilibrium. Based on the analysis in Section 2, we find that the equilibrium traffic pattern switches from Scenario 1 to Scenario 2, with the increase in the allocated capacity τ. At the transition point, we have $\beta = \lambda\frac{w(s+\tau)}{m} + \lambda\frac{2\tau}{s-\tau}$, i.e. $\tau = \tau^* = \frac{(2\lambda+\beta)-\sqrt{(2\lambda+\beta)^2-4\frac{\lambda ws}{m}\left(\beta-\frac{\lambda ws}{m}\right)}}{2\frac{\lambda w}{m}}$. We first investigate how the total system travel cost varies with capacity allocation in Scenario 1. We take the first-order derivative of $TSTC_{UE,1}$ with respect to the variable τ:

$$\frac{dTSTC_{UE,1}}{d\tau} = \frac{\beta N^2}{(\beta+\gamma)(s+\tau)^2}\left(4\lambda\tau^2\cdot\frac{1}{(s-\tau)^2} + 2\lambda\cdot\frac{s+\tau}{s-\tau} - \gamma\right). \tag{40}$$

Based on (40), we have *Proposition 4.1.* The proof can be found in Appendix B.

Proposition 4.1. For Scenario 1, we have: (i) when $\lambda \geq \frac{\gamma}{2}$, it is preferable to let $\tau \to 0$, i.e. $\tau_{UE} = 0$ (we denote τ_{UE} as the optimal capacity allocation solution at UE); when $0 < \lambda < \frac{\gamma}{2}$, it is preferable to let $\tau \to s\cdot\frac{\gamma-2\sqrt{\lambda(\gamma-\lambda)}}{\gamma-2\lambda}$, i.e. $\tau_{UE} = s\cdot\frac{\gamma-2\sqrt{\lambda(\gamma-\lambda)}}{\gamma-2\lambda}$.

As per Proposition 4.1, when $\lambda \geq \frac{\gamma}{2}$, we have $min\{TSTC_{UE,1}\} = \left[\frac{\beta N}{\beta+\gamma}\left(\frac{\lambda w}{m} + \frac{\gamma}{s}\right)\right]N$ with the optimal solution is $\tau_{UE} = 0$ (no capacity transfer) for the equilibrium AV traffic pattern under Scenario 1. This is explained as follows. When the value of λ is relatively large, it means that the AV self-driving activity becomes costly. As the proposed capacity allocation scheme reduces the service capacity of the outbound bottleneck, resulting in the increase in the queue time during the AV self-driving activity, the queuing delay cost at the outbound bottleneck could increase in a significant manner with τ under a large value of λ. This can be further justified by checking the first-order derivative of the total queuing delay cost at the outbound bottleneck TQ_2 in terms of τ, i.e. $\frac{dTQ_2}{d\tau} = \lambda N^2\frac{s^2+\tau^2}{(s^2-\tau^2)^2}$. It can be readily seen that $\frac{dTQ_2}{d\tau}$ is positive and expands with λ. Therefore, with a relatively large λ, the increase in τ could lead to the increase in the system-level travel cost.

When $0 < \lambda < \frac{\gamma}{2}$, we have $min\{TSTC_{UE,1}\} = \left[\frac{\beta N}{\beta+\gamma}\left(\frac{\lambda w}{m} + \frac{2\lambda\tau}{s^2\cdot\left(1-\left(\frac{\gamma-2\sqrt{\lambda(\gamma-\lambda)}}{\gamma-2\lambda}\right)^2\right)} + \frac{\gamma}{s\cdot\frac{2\gamma-2\lambda-2\sqrt{\lambda(\gamma-\lambda)}}{\gamma-2\lambda}}\right)\right]N$, with the optimal solution as $\tau_{UE} = \tau' = s\cdot\frac{\gamma-2\sqrt{\lambda(\gamma-\lambda)}}{\gamma-2\lambda}$ for the equilibrium AV traffic pattern under Scenario 1. This means that the total system travel cost can be reduced with regards to no capacity transfer (the initial case). However, after certain critical point τ', the $TSTC_{UE,1}$ turns out to increase with τ. There are two primary reasons for this. First, the increase of τ directly causes the decrease of the service capacity of the outbound bottleneck, which is equal to $(s-\tau)$. This could lead to an increase in the queuing delay cost when AVs experience traffic congestion during cruise-for-parking via self-driving. Second, when the transferred capacity τ increases further, the abovementioned congestion at the outbound capacity could become more severe. To avoid the high delay cost at the outbound bottleneck, AV commuters are incentivised to depart from home earlier, which results in a greater schedule delay cost for early arrival.

We then investigate the change of total system travel costs against capacity allocation in Scenario 2 by checking the first-order derivative of $TSTC_{UE,2}$ with respect to τ:

$$\frac{dTSTC_{UE,2}}{d\tau} = \frac{\beta\lambda N^2}{(\beta+\lambda)(s-\tau)^2}. \tag{41}$$

It can be readily verified that $\frac{dTSTC_{UE,2}}{d\tau} > 0$ always holds within the domain $\tau \in [0, s]$, which means that the system-level travel cost increases with the transferred capacity. This can be explained as follows. In Scenario 2, no congestion occurs at the inbound bottleneck, regardless of the value of τ. Therefore, the increase of τ cannot help improve the traffic condition at the inbound bottleneck. However, a further increase in τ reduces the service capacity of the outbound bottleneck, wherein a larger queuing delay is caused. This results in the increase in the total system travel cost.

With the above results in mind, we can investigate the optimal capacity allocation scheme in three different situations, denoted as Situations (i), (ii) and (iii), in the following subsections.

4.1.1 Situation (i)

For Situation (i), we consider $\lambda \geq \frac{\gamma}{2}$. Under this condition, the total system travel cost first increases with τ in Scenario 1, and then continue the increase in Scenario 2. In the meantime, the evaluation of $TSTC$ changes smoothly around the transition point $\tau = \frac{(2\lambda+\beta)-\sqrt{(2\lambda+\beta)^2-4\frac{\lambda ws}{m}\left(\beta-\frac{\lambda ws}{m}\right)}}{2\frac{\lambda w}{m}}$, as discussed earlier. Hence, in Situation (i), the optimal capacity allocation solution under user equilibrium is $\tau_{UE} = 0$, where the total system travel cost reaches the minimum, i.e. $min\{TSTC_{UE}\} = \left[\frac{\beta N}{\beta+\gamma}\left(\frac{\lambda w}{m}+\frac{\gamma}{s}\right)\right]N$.

4.1.2 Situation (ii)

For Situation (ii), we consider the condition $\lambda < \frac{\gamma}{2}$ and the following case: the total system travel cost decreases with τ in Scenario 1, and then increases with τ in Scenario 2. In this situation, we have the optimal capacity allocation solution $\tau_{UE} = \tau^* = s \cdot \frac{(2\lambda+\beta)-\sqrt{(2\lambda+\beta)^2-4\frac{\lambda ws}{m}\left(\beta-\frac{\lambda ws}{m}\right)}}{2\frac{\lambda ws}{m}}$ under user equilibrium, and the minimum total system travel cost $min\{TSTC_{UE}\} = \left[\frac{\lambda\left(\frac{w(s+\tau)}{m}+\frac{2\tau}{s-\tau}\right)\left(\frac{w}{m}+\frac{1}{s-\tau}\right)}{1+\frac{w(s+\tau)}{m}+\frac{2\tau}{s-\tau}}N\right]N$. It is noteworthy that, to ensure that Situation (ii) occurs, we need to add another condition $\tau^* \leq \tau'$, i.e. $\beta \leq \lambda\frac{w(s+\tau')}{m}+\lambda\frac{2\tau'}{s-\tau'}$. By substituting $\tau' = s \cdot \frac{\gamma-2\sqrt{\lambda(\gamma-\lambda)}}{\gamma-2\lambda}$, we then have $\beta \leq \lambda\left(\frac{2ws\left(\gamma-\lambda-\sqrt{\lambda(\gamma-\lambda)}\right)}{m(\gamma-2\lambda)}+\frac{\gamma-2\sqrt{\lambda(\gamma-\lambda)}}{\sqrt{\lambda(\gamma-\lambda)}-\lambda}\right)$.

We can find that the optimal capacity allocation scheme is influenced by the parking density m in Situation (ii). Furthermore, we have $\frac{d\tau_{UE}}{dm} > 0$, which means that the optimal transferred capacity becomes larger with the increase in m. This is explained as follows. Under Situation (ii), as the optimal solution is at the transition point between Scenario 1 and Scenario 2, the departure rate for early arrival is equal to the service capacity of the inbound bottleneck, i.e. $f_e = s + \tau$, without bottleneck congestion, and in the meantime, there is no late arrival under the derived equilibrium traffic pattern. In terms of parking choice, the parking location is determined by the departure time, and an earlier departure will yield a smaller AV self-driving cost due to

parking closer to the city centre. A larger parking density m indicates a more concentrated parking distribution over space and a smaller AV self-driving distance on average. Hence, with a larger parking density, commuters are less motivated to depart from home earlier, and instead, they would prefer to depart around the official work start time to reduce the schedule delay. Hence, a larger parking density leads to a more concentrated departure with a greater departure rate f_e. To derive the abovementioned optimal traffic pattern at equilibrium, the value of τ is to be increased, which ensures that the relationship $f_e = s + \tau$ holds.

4.1.3 Situation (iii)

For Situation (iii), we consider the condition $\lambda < \frac{\gamma}{2}$ and the following case: the total system travel cost first decreases and then increases with τ in Scenario 1, and then continues increasing with τ in Scenario 2. In this situation, we have the optimal capacity allocation solution $\tau_{UE} = \tau' = s \cdot \frac{\gamma - 2\sqrt{\lambda(\gamma-\lambda)}}{\gamma - 2\lambda}$, and the minimum total system travel cost $min\{TSTC_{UE}\} = \left[\frac{\beta N}{\beta+\gamma}\left(\frac{\lambda w}{m} + \frac{2\lambda\tau}{s^2\cdot\left(1-\left(\frac{\gamma-2\sqrt{\lambda(\gamma-\lambda)}}{\gamma-2\lambda}\right)^2\right)} + \frac{\gamma}{s\cdot\frac{2\gamma-2\lambda-2\sqrt{\lambda(\gamma-\lambda)}}{\gamma-2\lambda}}\right)\right]N$.

Similar to Situation (ii), a necessary condition for Situation (iii) is $\tau^* > \tau'$, i.e. $\beta > \lambda\left(\frac{2ws\left(\gamma-\lambda-\sqrt{\lambda(\gamma-\lambda)}\right)}{m(\gamma-2\lambda)} + \frac{\gamma-2\sqrt{\lambda(\gamma-\lambda)}}{\sqrt{\lambda(\gamma-\lambda)}-\lambda}\right)$.

We can find that the value of the optimal transferred capacity τ_{UE} is not directly influenced by the AV parking density m in Situation (iii). This is because in this situation, the optimal capacity allocation scheme leads to the equilibrium traffic pattern of Scenario 1, and it is readily to verify that τ and m have no direct interaction for the evaluation of $TSTC_{UE,1}$ (refer to Eq. (19)). However, this does not mean that the optimal τ has no relationship with the parking density in this context. This is explained as follows. To ensure that Situation (iii) occurs, that is Scenario 1 appears with the optimal τ, m should be sufficiently large, given that, as discussed earlier, a larger m could result in a more concentrated departure from home around the official work time. This would cause the queuing delay at the inbound bottleneck, which is the condition for the equilibrium traffic pattern of Scenario 1. Hence, a relatively large parking density m is the necessity for Situation (iii), which can also

be justified by the condition $\beta > \lambda\left(\frac{2ws\left(\gamma-\lambda-\sqrt{\lambda(\gamma-\lambda)}\right)}{m(\gamma-2\lambda)}+\frac{\gamma-2\sqrt{\lambda(\gamma-\lambda)}}{\sqrt{\lambda(\gamma-\lambda)}-\lambda}\right)$ for Situation (iii) (assuming that m is a variable, it should be sufficiently large to get this condition satisfied).

To summarise, the optimal capacity allocation solutions under user equilibrium traffic pattern in different situations are listed in Table 1. Note that, by referring to the existing literature where the bottleneck capacity is represented by a continuous term (Arnott et al., 1993; Xiao et al., 2012; Xiao et al., 2021), we derive the optimal solution based on a continuous variable τ in theory. In real-world practice, we may use a discrete value of τ. Under this circumstance, if the derived optimal solution τ_{UE} is not an integer or within the domain T containing the feasible discrete values, the nearest values around τ_{UE} within T should be selected as the optimal solution. This is primarily because, for Situations (ii) and (iii) where the optimal τ is not zero, we can prove the convexity of the system-level travel cost with respect to τ. This also applies to the SO situation as discussed in Section 4.2.

Table 1. Summary of optimal capacity allocation solutions for UE

Situation	Conditions	Optimal Solution
Situation (i)	$\lambda \geq \frac{\gamma}{2}$	$\tau_{UE} = 0$
Situation (ii)	$\lambda < \frac{\gamma}{2}$, and $\frac{\lambda ws}{m} < \beta \leq \lambda\left(\frac{2ws\left(\gamma-\lambda-\sqrt{\lambda(\gamma-\lambda)}\right)}{m(\gamma-2\lambda)}+\frac{\gamma-2\sqrt{\lambda(\gamma-\lambda)}}{\sqrt{\lambda(\gamma-\lambda)}-\lambda}\right)$	$\tau_{UE} = s \cdot \frac{(2\lambda+\beta)-\sqrt{(2\lambda+\beta)^2-4\frac{\lambda ws}{m}\left(\beta-\frac{\lambda ws}{m}\right)}}{2\frac{\lambda ws}{m}}$
Situation (iii)	$\lambda < \frac{\gamma}{2}$, and $\beta > \lambda\left(\frac{2ws\left(\gamma-\lambda-\sqrt{\lambda(\gamma-\lambda)}\right)}{m(\gamma-2\lambda)}+\frac{\gamma-2\sqrt{\lambda(\gamma-\lambda)}}{\sqrt{\lambda(\gamma-\lambda)}-\lambda}\right)$	$\tau_{UE} = s \cdot \frac{\gamma-2\sqrt{\lambda(\gamma-\lambda)}}{\gamma-2\lambda}$

It is worth mentioning that, for Situations (i) and (iii), commuters experience the queuing delay at both the inbound and outbound bottlenecks under the corresponding optimal capacity allocation schemes (i.e. the equilibrium traffic pattern is formed under Scenario 1). Differently, for Situation (ii), the departure rate from home is equal to the enhanced service capacity of the inbound bottleneck under the optimal capacity allocation scheme, and as a result, traffic congestion occurs at the outbound bottleneck only (i.e. the equilibrium traffic pattern is formed under Scenario 2).

4.2 Optimal capacity allocation under system optimum

We now turn to investigate the optimal capacity allocation scheme under the system-optimum traffic pattern in the fully autonomous environment. We denote τ_{SO} as the optimal capacity allocation solution at system optimum, and have Proposition 4.2. The proof can be found in Appendix B.

Proposition 4.2. When $\lambda \geq \frac{\beta\gamma}{2\beta+\gamma}$, it is preferable to let $\tau \to 0$, i.e. $\tau_{SO} = 0$; When $\lambda < \frac{\beta\gamma}{2\beta+\gamma}$, we have $\tau_{SO} = \left(\sqrt{\frac{(\gamma-\lambda)\beta}{\lambda(\beta+\gamma)}} - 1\right) \cdot s / \left(\sqrt{\frac{(\gamma-\lambda)\beta}{\lambda(\beta+\gamma)}} + 1\right)$.

Based on Proposition 4.2., when $\lambda \geq \frac{\beta\gamma}{2\beta+\gamma}$, we have the minimum total system travel cost at SO as $min\{TSTC_{SO}\} = \beta \cdot \left[0.5 \cdot \left(\frac{\gamma}{\beta+\gamma}\right)^2 \frac{N^2}{s}\right] + \gamma \cdot \left[0.5 \cdot \left(\frac{\beta}{\beta+\gamma}\right)^2 \frac{N^2}{s}\right] + \lambda \cdot \left[0.5\frac{w}{m}N^2\right]$ under $\tau_{SO} = 0$. When $\lambda < \frac{\beta\gamma}{2\beta+\gamma}$, we have $min\{TSTC_{SO}\} = \beta \cdot \left[\frac{\lambda^2}{(\lambda+\beta)^2}\left(\sqrt{\frac{(\gamma-\lambda)\beta}{\lambda(\beta+\gamma)}} + 1\right)\frac{N^2}{4s} + \frac{(\gamma-\lambda)\beta}{(\lambda+\beta)(\beta+\gamma)(s+\tau)}\left(\sqrt{\frac{\lambda(\beta+\gamma)}{(\gamma-\lambda)\beta}} + 1\right)\left(\frac{\lambda}{\lambda+\beta} + \frac{\gamma}{\beta+\gamma}\right)\frac{N^2}{4s}\right] + \gamma \cdot \left[\left(\frac{\beta}{\beta+\gamma}\right)^2\left(\sqrt{\frac{\lambda(\beta+\gamma)}{(\gamma-\lambda)\beta}} + 1\right)\frac{N^2}{4s}\right] + \lambda \cdot \left[\left(\frac{\beta}{\lambda+\beta}\right)^2\left(\sqrt{\frac{(\gamma-\lambda)\beta}{\lambda(\beta+\gamma)}} - \sqrt{\frac{\lambda(\beta+\gamma)}{(\gamma-\lambda)\beta}}\right)\frac{N^2}{4s}\right] + \lambda \cdot \left[0.5\frac{w}{m}N^2\right]$ under $\tau_{SO} = \left(\sqrt{\frac{(\gamma-\lambda)\beta}{\lambda(\beta+\gamma)}} - 1\right) \cdot s / \left(\sqrt{\frac{(\gamma-\lambda)\beta}{\lambda(\beta+\gamma)}} + 1\right)$.

The optimal capacity allocation scheme for SO traffic pattern exhibits some similarities to that for the UE traffic pattern for the AV morning commute. Particularly, when the value of unit time for AV self-driving is relatively large, the transfer of capacity from the inbound direction to the outbound direction would increase the system-level travel cost. This is primarily because a large λ indicates costly AV self-driving, while capacity transfer would increase the queuing delay during the self-driving activity at the outbound bottleneck. Thus, we have $\tau_{SO} = 0$ for the optimal capacity allocation scheme under this circumstance. When the value of unit time for AV self-driving is relatively small, the system-level travel cost would first decrease and then increase against the transferred capacity (please refer to Proof. Proposition 4.2. in Appendix B), so we have the optimal capacity allocation scheme with a medium value of τ within the domain $(0, s)$.

Different from the optimal solution τ_{UE}, τ_{SO} does not have any relationship with the AV parking density in any case. This is explained as follows. Under the SO commuting pattern, only one travel cost component is affected by the AV parking density, which is the total travel cost of AV self-driving for the parking purpose under

the free-flow condition, denoted as TP_{SO}. Meanwhile, the TP_{SO} is a fixed term with a given m, which is independent of the transferred capacity τ. Given this, for the optimal capacity allocation solution under SO, we indeed find a τ that minimises the sum of the total schedule delay cost and the total queueing delay cost. However, none of them is influenced by m, since under the SO conditions, the departure time and rate are independent of the parking density m. Based on the above analysis, the AV parking density does not affect the optimal solution τ_{SO}.

5 Numerical Studies

In this section, we conduct some numerical studies to illustrate the analytical models. Firstly, we analyse the AV traffic pattern under UE and SO in multiple scenarios, as well as different system cost measures against the AV parking supply. Secondly, we investigate the optimal capacity allocation scheme, which aims to minimise the system-level travel cost.

5.1 System efficiency metrics

In this section, we conduct sensitivity analysis of several system efficiency metrics against the AV parking density, which includes different types of schedule delay costs, queuing delay costs and self-driving costs. We also analyse the system-level travel costs both at UE and SO. By referring to the existing literature (Zhu et al., 2019; Tang et al., 2021; Xiao et al., 2021), we set the values of parameters used in this subsection for the demonstration purpose, as summarised in Table 2. Note that, for real-world practice, the setting of these parameters depends on case-by-case empirical findings and field investigations for a city or community. As shown in Table 2, this subsection includes three cases, which indicate the UE traffic patterns under different scenarios. The results obtained from our proposed models are summarised in Figure 5 and Figure 6.

Table 2. Parameters used for numerical studies (I)

Parameter	Case 1	Case 2	Case 3
α (\$/h)	9.91	9.91	9.91
β (\$/h)	6.00	6.00	6.00
γ (\$/h)	17.00	17.00	17.00
λ (\$/h)	4.00	4.00	4.00
s (veh/h)	4000	4000	4000
τ (veh/h)	500	1750	1600
w (h/km)	0.025	0.025	0.025
N (veh)	3,500	3,500	3,500
m (space/km)	[150,1500]	[150,1500]	[150,1500]
No. of Scenario at UE	1	2	1 and 2

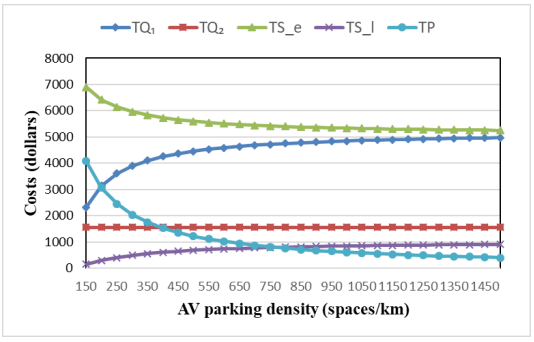

(a) Case 1

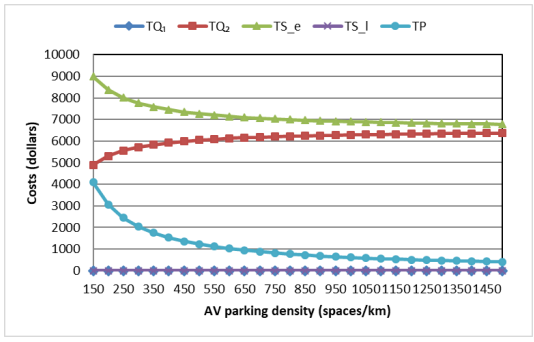

(b) Case 2

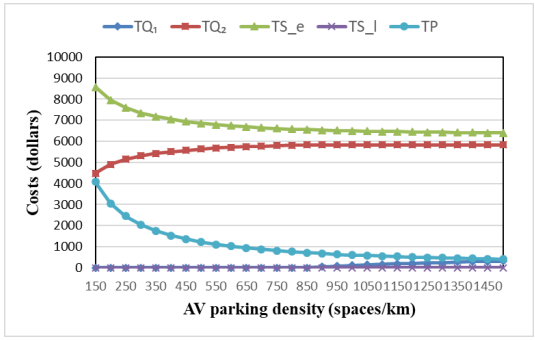

(c) Case 3

Figure 5. Efficiency metrics against parking density under capacity allocation schemes

Figure 5 displays five efficiency metrics at user equilibrium in Cases 1,2 and 3, which represent the equilibrium AV traffic pattern under certain capacity allocation schemes in different scenarios. Specifically, the UE traffic patterns in Case 1 and Case

2 are respectively formed under Scenario 1 and Scenario 2, while in Case 3 the UE traffic pattern switches from Scenario 2 to Scenario 1 around the transition point $m = 800$.

For all the three cases, the total schedule delay cost for early arrival decreases with the increase in the AV parking density. This is because a larger m indicates a more concentrated parking distribution, which means that the difference in AV self-driving distance becomes less significant. Given this, commuters are less motivated to depart from home earlier to get an advantageous parking space that is closer to the workplace. This can be further verified by taking the first-order derivative $\frac{d(t^*-t_s)}{dm}$. By substituting Eq. (15) and Eq. (32), it can be easily seen that $\frac{d(t^*-t_s)}{dm} < 0$ holds. This means that the start time of morning commute becomes closer to the official work start time with the increase in m under the capacity allocation scheme, leading to the reduction in the TS_e. However, this change will make more commuters depart from home around t^*, which leads to the increase in the total queuing delay cost at the inbound bottleneck for Case 1, as shown in Figure 5 (a). Different from Case 1, the TQ_1 is always equal to zero in Case 2, since no traffic congestion occurs at the inbound bottleneck at equilibrium in Scenario 2. Hence, in Case 3, TQ_1 first remains zero under Scenario 2 and then increase under Scenario 1, which changes smoothly around the transition point. Furthermore, in Scenario 2, every commuter arrives at the workplace early or on time in the morning under the given capacity allocation scheme, so there is no schedule delay cost for late arrival, which is different from the equilibrium traffic pattern under Scenario 1 and that with no capacity allocation.

By comparing Case 1 and Case 2, we find that a larger allocated capacity τ can cause the UE traffic pattern to switch from Scenario 1 to Scenario 2. This phenomenon can be explained as follows. When we transfer more capacity from the outbound bottleneck to the inbound bottleneck, the cost for queuing delay at the outbound bottleneck tends to become larger under poorer service capacity. Consequently, the marginal saving in the early schedule delay cost by postponing a unit departure time becomes smaller than the marginal increase in the cost of cruising-for-parking via AV self-driving under traffic congestion at the outbound bottleneck. Under such situation, commuters would prefer to depart from home earlier in the morning to avoid significant queuing delay at the outbound direction. With more disperse departure from home and larger inbound bottleneck capacity, the traffic congestion does not occur at the inbound direction, leading to Scenario 2.

From Figure 5, it can be seen that traffic congestion occurs at the outbound bottleneck under AV traffic patterns at UE, i.e. $TQ_2 > 0$. This is one of the major differences from Liu (2018) and Zhang et al. (2019) where the capacity allocation strategy is not considered. This is primarily because under the capacity allocation scheme, the transport facility is asymmetric, i.e. the capacity of the inbound bottleneck $(s + \tau)$ becomes greater than that of the outbound bottleneck $(s - \tau)$. This means that the arrival rate to the outbound bottleneck can be increased beyond its service capacity, which causes the queuing delay. Specifically, in Case 1, as the service rate of the inbound bottleneck is at capacity under Scenario 1, the rate of arrival at the outbound capacity is always equal to $(s + \tau)$ with the departure rate as $(s - \tau)$ under the given total travel demand, so that the total cost of queuing delay at the outbound bottleneck remains unchanged regardless of the AV parking density. By contrast, in Case 2, the arrival rate of the outbound bottleneck is the same as that of the inbound bottleneck as well as the departure rate from home (f_e in Eq. (31)) under Scenario 2, given that no congestion occurs at the inbound bottleneck under the capacity allocation scheme. Moreover, this arrival rate becomes greater with a larger m since people are incentivised to depart from home close to t^*, as discussed earlier (also, as per Eq. (31), we have $\frac{df_e}{dm} > 0$). With the increasing arrival rate to the outbound bottleneck, the TQ_2 becomes larger against m, as shown in Figure 5(b). This also explains why TQ_2 first increases and then remains unchanged in Case 3 where the UE traffic pattern switches from Scenario 2 to Scenario 1.

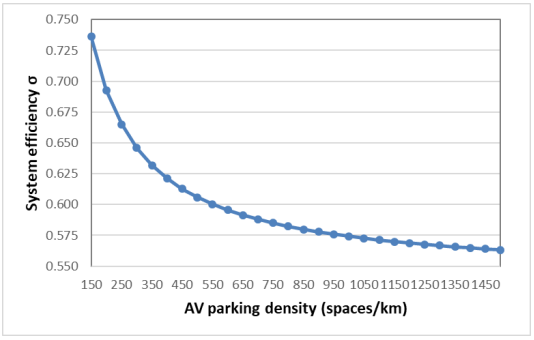

(a) Case 1

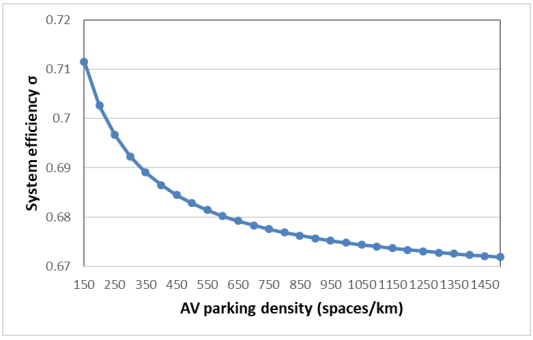

(b) Case 2

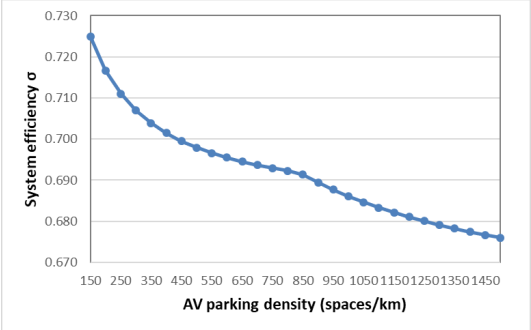

(c) Case 3

Figure 6. Relative system efficiency against parking density under capacity allocation schemes

In Figure 6, we display the relative system efficiency σ against the parking density m. It can be found that the relative system efficiency is decreasing with the parking density m. This means that, by providing more parking spaces that are close to the workplace, the system optimum becomes more efficient against the user equilibrium, when a capacity allocation scheme applies to AV morning commutes. This is explained as follows. The increase in the parking density m leads to a reduction in the total cost for cursing-for-parking via self-driving under the free-flow condition, both for UE and SO. With the increase in m, the total queuing delay cost remains unchanged at SO. However, for UE, it increases for either inbound bottleneck (Scenario 1) or outbound bottleneck (Scenario 2), leading to the decrease in σ. Furthermore, it can be seen in Figure 6 (c) that the curve descends abruptly at the transition point $m = 800$. This is primarily because when the scenario switches from Scenario 2 to Scenario 1, both the queuing delay cost in the inbound direction and the schedule delay cost for late arrival come up, and then become larger with the parking density.

5.2 Capacity allocation scheme

In this section, we investigate the optimal capacity allocation scheme for AVs, and explore the insights into the impacts of capacity allocation on the AV traffic pattern. We conduct four case studies, and the numerical setting are listed in Table 3. Note that the value of τ increases from 0 to 3,975 with an interval of 25 in this numerical experiment. The results are depicted in Figure 7.

Table 3. Parameters used for numerical studies (II)

Parameter	Case 4	Case 5	Case 6	Case 7
α (\$/h)	5.5	15	15	15

β (\$/h)	4.5	2.5	2.5	10
γ (\$/h)	7	17	17	17
λ (\$/h)	4	2	0.7	2
s (veh/h)	4000	4000	4000	4000
τ (veh/h)	[0, 3975]	[0, 3975]	[0, 3975]	[0, 3975]
w (h/km)	0.025	0.025	0.025	0.025
N (veh)	3500	3500	3500	3500
m (space/km)	1000	1000	1000	1000

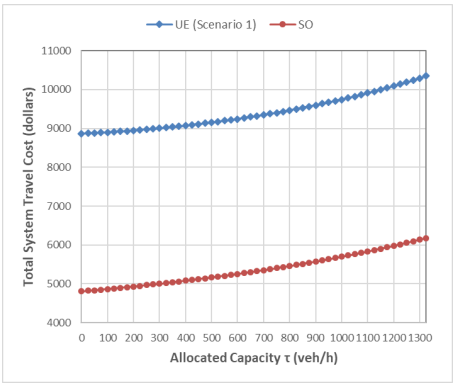

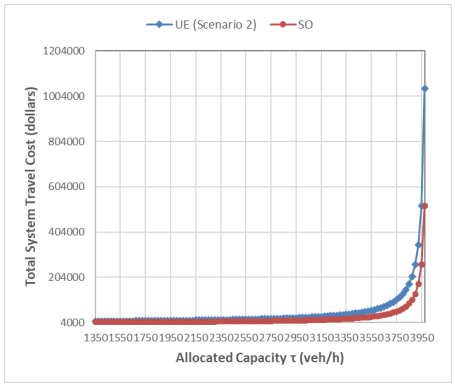

(a) Case 4: $\lambda > \frac{\gamma}{2}$

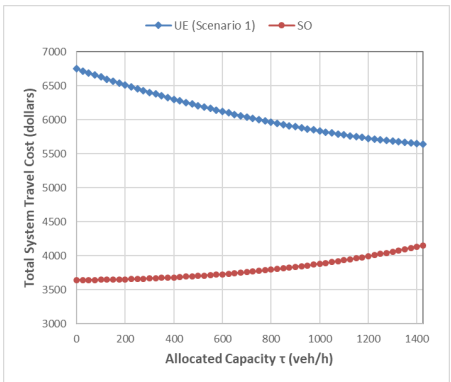

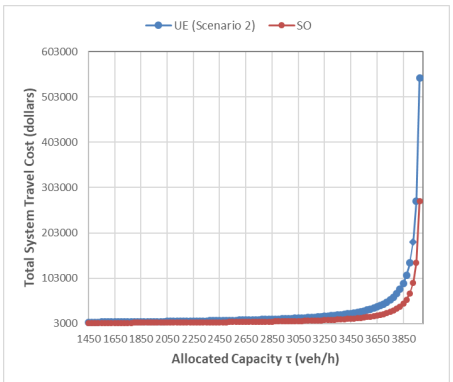

(b) Case 5: $\frac{\beta\gamma}{2\beta+\gamma} \le \lambda < \frac{\gamma}{2}$, $\frac{\lambda ws}{m} < \beta \le \lambda\left(\frac{2ws\left(\gamma-\lambda-\sqrt{\lambda(\gamma-\lambda)}\right)}{m(\gamma-2\lambda)} + \frac{\gamma-2\sqrt{\lambda(\gamma-\lambda)}}{\sqrt{\lambda(\gamma-\lambda)}-\lambda}\right)$

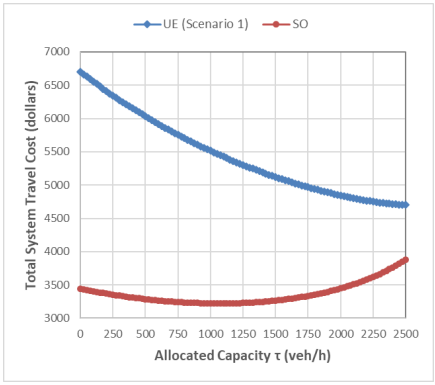

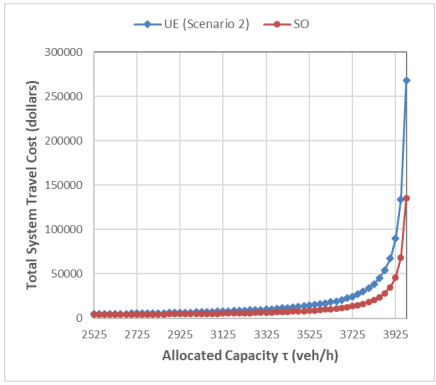

(c) Case 6: $0 < \lambda < \frac{\beta\gamma}{2\beta+\gamma}$, $\frac{\lambda ws}{m} < \beta \le \lambda\left(\frac{2ws\left(\gamma-\lambda-\sqrt{\lambda(\gamma-\lambda)}\right)}{m(\gamma-2\lambda)} + \frac{\gamma-2\sqrt{\lambda(\gamma-\lambda)}}{\sqrt{\lambda(\gamma-\lambda)}-\lambda}\right)$

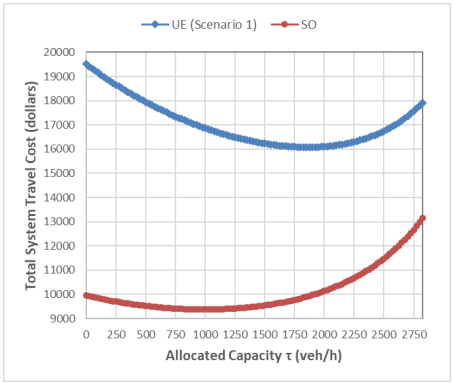

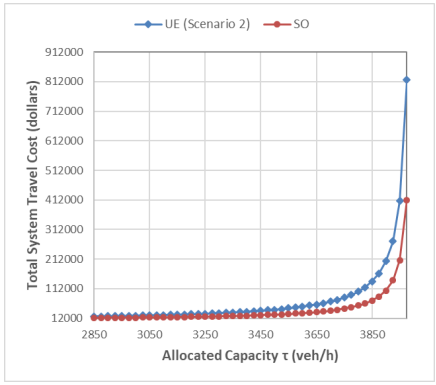

(d) Case 7: $0 < \lambda < \frac{\beta\gamma}{2\beta+\gamma}$; $\beta > \lambda\left(\frac{2ws\left(\gamma-\lambda-\sqrt{\lambda(\gamma-\lambda)}\right)}{m(\gamma-2\lambda)} + \frac{\gamma-2\sqrt{\lambda(\gamma-\lambda)}}{\sqrt{\lambda(\gamma-\lambda)}-\lambda}\right)$

Figure 7. Total system travel cost against capacity allocation for AV morning commute

For all the four cases, we can see that the UE traffic pattern switches from Scenario 1 to Scenario 2 when the allocated capacity τ increases. This is explained as follows. Initially, when $\tau = 0$, $\beta > \lambda\frac{w(s+\tau)}{m} + \lambda\frac{2\tau}{s-\tau}$ holds, given that we have $\beta > \lambda\frac{ws}{m}$. This means that by postponing a unit of departure time, the saving in the early schedule delay cost is greater than the increase in the cruising-for-parking cost that considers both the parking location and the delay during the AV self-driving process. In this case, more people are motivated to depart from home when it is close to the official working time t^*, in order to reduce the early schedule delay cost. This causes more concentrated departures, resulting in congestion at the inbound bottleneck, where the equilibrium traffic pattern is formed under Scenario 1. With the expansion in τ, relationship between β and the term $\lambda\frac{w(s+\tau)}{m} + \lambda\frac{2\tau}{s-\tau}$ changes to $\beta < \lambda\frac{w(s+\tau)}{m} +$

$\lambda\frac{2\tau}{s-\tau}$, given that the latter is monotonically increasing with τ. With such a relationship, the marginal saving in the early schedule delay cost becomes less than the increase in the total cost for the cruising-for-parking activity, because of the relatively insufficient service capacity at the outbound bottleneck. Therefore, commuters are incentivised to depart from home earlier to avoid the high cost for the AV parking activity. This causes less concentrated departures along with the expanded service capacity of the inbound direction. As a result, the queuing delay at the inbound bottleneck is eliminated, and the equilibrium traffic pattern is formed under Scenario 2. Different from UE, no queuing delay occurs at the inbound bottleneck under the SO conditions, and the SO traffic pattern does not switch from one scenario to another with the increase in τ.

In Case 4, we have a relatively large value of time for AV self-driving, i.e. $\lambda > \frac{\gamma}{2}$. In this case, the cost of cruising for parking via AV self-driving increases rapidly with the delay occurred at the outbound bottleneck, and this delay expands with the transferred capacity τ. Hence, the total system travel cost in increasing with τ, both at UE and at SO, and we then have $\tau_{UE} = \tau_{SO} = 0$.

Case 5 is a medium case, where we have $\frac{\beta\gamma}{2\beta+\gamma} \leq \lambda < \frac{\gamma}{2}$. The SO traffic pattern is similar to that in Case 4, where the total system travel cost is monotonically increasing with the allocated capacity. Therefore, we still have $\tau_{SO} = 0$. By contrast, the system-level travel cost decreases at the beginning for the UE traffic pattern. The primary reason is that the total cost of queuing delay in the inbound direction is reduced due to the expanded capacity of the inbound bottleneck. This shares some similarity with Case 6, which will be discussed later.

When the AV self-driving is not costly, we investigate the sensitivity of total travel cost to the capacity allocation scheme in Case 6 and Case 7. For Case 6, we find that the total system travel cost at equilibrium decreases when a relatively small capacity is transferred to the inbound direction in Scenario 1. After the capacity allocation exceeds 2,500 veh/h, the equilibrium traffic pattern switches to Scenario 2, where the total system travel cost increases with τ. Hence, in Case 6, the optimal capacity allocation scheme should be $\tau_{UE} = 2500\text{veh/h}$. Different from Case 6, for Case 7, the total system travel at equilibrium first decreases and then increases in Scenario 1, where the transitional point is around 1850 veh/h. When the allocated capacity τ exceeds 2850 veh/h, the traffic pattern switches from Scenario 1 to Scenario 2, and the $TSTC$ continues increasing. Hence, we have $\tau_{UE} = 1850\ \text{veh/h}$ in Case 7. Furthermore, we note that, for both Case 6 and Case 7, when the allocated

capacity is approaching the service capacity s, the total system travel cost increases with τ in a drastic manner. There are two main reasons for this phenomenon. One is that the low service capacity of the outbound direction due to the increased τ has caused severe traffic congestion when AVs cruise for parking via self-driving. This leads to a large queuing delay cost at the outbound bottleneck. The second reason is that considering the poor service quality of the outbound direction, commuters are motivated to depart from home much earlier to avoid the terrible queuing delay at the outbound bottleneck, which results in a significant increase in the total schedule cost for early arrival.

For both Case 6 and Case 7, the total system travel cost first decreases and then increases with the allocated capacity τ under the SO condition. It is noteworthy that for the optimal capacity allocation schemes, we have $\tau_{SO} < \tau_{UE}$. This is explained as follows. At UE, there is a queue in the inbound direction in Scenario 1, so more allocated capacity could help further reduce the total cost of queuing delay at the inbound bottleneck. By contrast, for SO, the relationship $f \leq s + \tau$ always holds as per our analysis in Section 3. This means that traffic congestion will never occur at the inbound bottleneck under the SO condition. Hence, an additional increase in the allocated capacity could mainly cause an increase in the queuing delay in the outbound direction when τ has become sufficiently large, leading to the increase in the system-level travel cost.

6 Conclusion

This study investigates the morning commute for autonomous vehicles (AVs) under the spatial capacity allocation schemes, where we may optimally transfer part of the service capacity from the outbound direction to the inbound direction in order to improve traffic efficiency. We develop the analytical model for multiple AV traffic patterns considering capacity allocation under user equilibrium (UE) and system optimum (SO). Furthermore, we derive the optimal capacity allocation strategies under different conditions. Finally, we conduct numerical studies to illustrate the proposed models and analysis.

This study is the first in the literature to investigate the AV commuting and parking pattern where both the parking activity via self-driving and the capacity allocation scheme are accounted for. In particular, this study contributes to the literature on morning commute analysis from the following two aspects. First, as compared to AV equilibrium analysis where no capacity allocation is considered (Liu, 2018; Zhang

et al., 2019a), we derive the different commuting and parking patterns in the AV environment, both for UE and SO conditions, under any capacity allocation scheme. The research outcome serves as a modelling device to quantify the impacts of capacity allocation options on the commuting behaviour and the system-level travel cost in the AV era. Based on this, we optimise the capacity allocation strategy to improve AV traffic efficiency. Second, as compared to research on capacity allocation for non-AVs (Xiao et al., 2016), the capacity allocation scheme here involves decision making of endogenously related potential road bottlenecks due to new AV behaviour features.

This study provides understanding into infrastructure and traffic management with the automated traffic, which is discussed below. (i) By examining the optimal spatial capacity allocation scheme, it is found that due to the AV-self driving and the interacted bottlenecks on two opposite directions, transferring service capacity from the outbound direction to the inbound during morning peaks does not necessarily improve the system efficiency. Particularly, when AV self-driving is costly, the reduced outbound bottleneck capacity could incur an increase in the system-level travel disutility because of the expanded queuing delay at the outbound bottleneck. When the AV self-driving cost rate is relatively small, allocating more capacity to the inbound direction can help improve traffic efficiency. (ii) We derive and compare the optimal capacity allocation schemes when the traffic pattern is under no-toll user equilibrium or the tolled system optimum. It is found that the optimal capacity allocation scheme under the tolled system optimum does not depend on the parking density or distribution, while that under no-toll user equilibrium can be affected by the parking density or distribution. This is because, at the no-toll equilibrium, the parking density will affect the departure/arrival rate and thus affect the congestion pattern, and the optimal capacity allocation should then incorporate the impact of parking supply. (iii) We propose the time-varying tolling scheme and the location-dependent parking pricing scheme, which derive the system optimum for AV morning commutes under capacity allocation.

This study can be extended in multiple directions. First, future studies may consider carpooling and shared parking for AVs, and how these might interact with the optimal spatial capacity allocation (Liu and Li, 2017; Su and Wang, 2020). Second, similar to Zhang et al. (2019a), the integrated morning-evening commuting pattern under capacity allocation for AVs can be investigated in a follow-up study, where the interaction between the two peak periods and how such interaction will affect the optimal capacity allocation and AV traffic patterns will be quantified. Third, to further improve the transport system performance, a temporal capacity allocation strategy can

be developed for AV commutes, where the allocated capacity can vary over different time periods. In this context, one then can investigate the equilibrium traffic patterns and the optimal capacity allocation scheme, and also evaluate the efficiency gain by allowing a time-dependent capacity allocation. Fourth, in this paper the road capacity is considered as a continuous variable and the allocations to inbound and outbound directions are also considered as continuous variables, which allow analytical derivations. While the exact numerical solutions will be different if the capacity is constrained to discrete values, we expect that the major understanding and insights generated in this paper will still hold. For capacity allocation scheme implementation in practice, a tactic or operational level model has to be further developed to incorporate discrete decision variables. Fifth, the searching radius of AVs for parking might be limited for safety and energy considerations, which is not considered in this study. For future studies with planning or operational level models, such factors can be incorporated. Furthermore, this study can be extended to heterogeneous users including both AV and non-AV commuters (Tian et al., 2019; Tang et al., 2021). In this extension, two potential behaviour patterns can be modelled simultaneously, i.e., "AVs drop off travellers + AVs self-drive for parking" and "AVs or non-AVs park + travellers walk to destination", where their interactions are to be explored under the capacity allocation scheme.

Appendix A. Notations

Table A.1 Mathematical notations

Notation	Definition
N	The total travel demand
t	The time of departure from home
t^*	The official work start time
t_s,t_e	The time of departure from home for the first and the last commuters
α	The cost for a unit time when commuters are driving AVs
β	The penalty cost for a unit time of early arrival at the workplace
γ	The penalty cost for a unit time of late arrival at the workplace
λ	The cost for a unit time when AVs drive themselves

w	The travel time needed to cover a unit distance by AV self-driving
s	The service capacity at the bottleneck
x	The distance to the workplace (city centre)
x_0	The distance between the workplace and the closest parking space to it
m	The parking density for autonomous vehicles
$q_1(t),\ q_2(t)$	The queue length at the inbound bottleneck and at the outbound bottleneck, respectively, experienced by commuters departing from home at t
$f(t)$	The departure rate from home at time t
$f_e,\ f_l$	The departure rates for early arrival and late arrival at equilibrium
τ	The capacity transferred from the outbound direction to the inbound direction
τ_{UE}, τ_{SO}	The optimal value of τ for user equilibrium and that for system optimum
$TQ_1,\ TQ_2$	The total cost of queuing delay experienced at the inbound bottleneck and at the outbound bottleneck, respectively
$TS_e,\ TS_l$	The total cost of schedule delay for early arrival and for late arrival, respectively
TS	The total cost of schedule delay
TP	The total cost for cruising-for-parking via AV self-driving without traffic congestion
TSD	The total cost of AV self-driving
$TSTC_{UE}$, $TSTC_{SO}$	The total system travel cost at user equilibrium and at system optimum, respectively

Appendix B. Proofs

B.1 Proof. Proposition 2.1.

Assuming that the arrival time to the workplace is later than t^* in Scenario 2, the travel disutility can be calculated as follows

$$c(t,x) = \gamma \cdot [t + T_1(t) - t^*]^+ + \lambda w x(t) + \lambda \cdot T_2(t), \tag{42}$$

where $T_1(t) = 0,\ T_2(t) = \frac{\int_{t_s}^{t} (f(v)-(s-\tau))^+ dv}{(s-\tau)}$.

We then have $\frac{dc(t,x)}{dt} = \gamma + \lambda \cdot w\frac{f(t)}{m} + \lambda \cdot \frac{f(t)}{s-\tau} - \lambda$. Given $\gamma > \alpha > \lambda$, the relationship $\frac{dc(t,x)}{dt} > 0$ must hold. This means that the total individual travel disutility for late arrivals must be greater than that for on-time arrivals, resulting in the disequilibrium. This proves that Proposition 2.1. is true. □

B.2 Proof. Proposition 3.1.

To prove the Proposition 3.1., we first investigate the departure pattern at system optimum. Second, we formulate the total system travel cost, and derive the values of the parameters under the SO conditions.

First, for early arrival, we aim to reduce the total schedule delay and the total queuing delay at the outbound bottleneck at system optimum. From Figure 4, the former can be represented by the area between the green curve PC and the dotted line CU' denoted as $\Omega_{s,e}$; the latter can be represented by the area between the green curve PC and the blue line PD denoted as $\Omega_{q,e}$. It can be seen that when the curve PC is formed in the manner that it consists of two straight lines, i.e. PBC where $f_{e,1} = s - \tau$ on PB and $f_{e,2} = s + \tau$ on BC, the areas $\Omega_{s,e}$ and $\Omega_{q,e}$ will reach their minimum simultaneously. This is because among all the feasible forms under the constraint $f \in [s-\tau, s+\tau]$, the PBC is located 'closest' both to CU' and to PD. Any other pattern for the curve PC (for instance, the straight line PC with a constant f_e) would simply expand both areas $\Omega_{s,e}$ and $\Omega_{q,e}$ under any given $t_{s,SO}$ and N_e. For late arrival, the sum of the total schedule delay and the total queuing delay always equals the area of the polygon $CDWU$ under the SO conditions. Note that for any given combination of $(t_{s,SO}, N_e)$, the polygon $CDWU$ has been determined regardless of the early departure pattern, subject to $f \in [s-\tau, s+\tau]$. To achieve the system optimum, the green curve CZ should approach the dotted line CU to the largest extent, in order to minimise the sum of the total schedule delay cost and the total queuing delay cost. This is because the penalty rate for late arrival is greater than the AV self-driving cost rate, i.e. $\gamma > \lambda$. Under this circumstance, we have $f_l = s + \tau$ for late arrival.

Second, to quantify the SO traffic pattern for AV commutes under capacity allocation, we investigate the system-level travel disutility under any given $t_{s,SO}$ and N_e. The total schedule delay cost for early arrival and late arrival at system optimum, denoted as $TS_{e,SO}$ and $TS_{l,SO}$ respectively, can be determined as follows:

$$TS_{e,SO} = \beta \cdot (\mathrm{A}_{PBB'} + \mathrm{A}_{BB'U'C}) = \beta \cdot \left[0.5 \cdot \left(\frac{(s+\tau)(t^* - t_{s,SO}) - N_e}{2\tau}\right)^2 \cdot (s-\tau) + 0.5 \cdot \left(\frac{(s+\tau)(t^* - t_{s,SO}) - N_e}{2\tau}(s-\tau) + N_e\right) \cdot \left(\frac{N_e - (s-\tau)(t^* - t_{s,SO})}{2\tau}\right)\right]; \quad (43)$$

$$TS_{l,SO} = \gamma \cdot A_{CUZ} = \gamma \cdot \left[0.5 \cdot \frac{(N-N_e)^2}{s+\tau}\right]. \quad (44)$$

The total schedule delay cost at system optimum, denoted as TS_{SO}, is:

$$TS_{SO} = TS_{e,SO} + TS_{l,SO} = \beta \cdot \left[0.5 \cdot \left(\frac{(s+\tau)(t^* - t_{s,SO}) - N_e}{2\tau}\right)^2 \cdot (s-\tau) + 0.5 \cdot \left(\frac{(s+\tau)(t^* - t_{s,SO}) - N_e}{2\tau}(s-\tau) + N_e\right) \cdot \left(\frac{N_e - (s-\tau)(t^* - t_{s,SO})}{2\tau}\right)\right] + \gamma \cdot \left[0.5 \frac{(N-N_e)^2}{s+\tau}\right]. \quad (45)$$

The total queuing delay cost at the outbound bottleneck can be determined as follows:

$$TQ_{2,SO} = \lambda \cdot A_{BZW} = \lambda \cdot \left[0.5 \cdot \left(N - \left(\frac{(s+\tau)(t^* - t_{s,SO}) - N_e}{2\tau}\right)(s-\tau)\right)^2 \left(\frac{2\tau}{s^2-\tau^2}\right)\right]. \quad (46)$$

The total cost for cruising-for-parking via AV self-driving under the free-flow condition can be determined as follows:

$$TP_{SO} = \lambda \cdot \left[0.5 \frac{w}{m} N^2\right]. \quad (47)$$

Then, the total system travel cost at system optimum $TSTC_{SO}$ under any given $t_{s,SO}$ and N_e can be calculated as follows:

$$TSTC_{SO} = TS_{SO} + TQ_{SO} = \beta \cdot \left[0.5 \cdot \left(\frac{(s+\tau)(t^* - t_{s,SO}) - N_e}{2\tau}\right)^2 \cdot (s-\tau) + 0.5 \cdot \left(\frac{(s+\tau)(t^* - t_{s,SO}) - N_e}{2\tau}(s-\tau) + N_e\right) \cdot \left(\frac{N_e - (s-\tau)(t^* - t_{s,SO})}{2\tau}\right)\right] + \gamma \cdot \left[0.5 \frac{(N-N_e)^2}{s+\tau}\right] + \lambda \cdot 0.5 \cdot \left(N - \left(\frac{(s+\tau)(t^* - t_{s,SO}) - N_e}{2\tau}\right)(s-\tau)\right)^2 \left(\frac{2\tau}{s^2-\tau^2}\right) + \lambda \cdot \left[0.5 \frac{w}{m} N^2\right]. \quad (48)$$

Based on Eq. (48), by taking the first-order derivative of $TSTC_{SO}$ with respect to the start time of departure from home $t_{s,SO}$, we have:

$$\frac{dTSTC_{SO}}{dt_{s,SO}} = \beta \left[\frac{\left(-(s^2-\tau^2)(t^* - t_{s,SO}) + N_e(s-\tau)\right)}{2\tau}\right] + \lambda \left[N - \left(\frac{(s^2-\tau^2)(t^* - t_{s,SO}) - N_e(s-\tau)}{2\tau}\right)\right]. \quad (49)$$

By taking the first-order derivative of $TSTC_{SO}$ with respect to the number of early arrivals N_e, we have:

$$\frac{dTSTC_{SO}}{dN_e} = \beta \cdot \frac{N_e}{2\tau} - \beta \frac{s-\tau}{2\tau}\left(t^* - t_{s,SO}\right) - \gamma \cdot \frac{N}{s+\tau} + \gamma \cdot \frac{N_e}{s+\tau} + \lambda \cdot \frac{N}{s+\tau} - \lambda \cdot \left(\frac{s-\tau}{2\tau}\right)\left(t^* - t_{s,SO}\right) + \lambda \cdot \left(\frac{s-\tau}{s+\tau}\right)\frac{N_e}{2\tau}. \tag{50}$$

Based on Eqs. (49) and (50), we have the second-order derivatives as follows:

$$\frac{d^2TSTC_{SO}}{dt_{s,SO}{}^2} = \beta \frac{1}{2\tau} \cdot (s^2 - \tau^2) + \lambda\left(\frac{(s^2-\tau^2)}{2\tau}\right) = (\beta + \lambda)\frac{1}{2\tau} \cdot (s^2 - \tau^2);$$

$$\frac{d^2TSTC_{SO}}{dN_e{}^2} = \frac{\beta}{2\tau} + \frac{\gamma}{s+\tau} + \lambda \cdot \left(\frac{s-\tau}{s+\tau}\right)\frac{1}{2\tau}; \tag{51}$$

$$\frac{d^2TSTC_{SO}}{dt_{s,SO}dN_e} = \frac{d^2TSTC_{SO}}{dN_e dt_{s,SO}} = (\beta + \lambda) \cdot \left(\frac{s-\tau}{2\tau}\right).$$

At the system optimum, the total system travel cost should reach its minimum, so the following conditions should get satisfied:

$$\frac{dTSTC_{SO}}{dt_{s,SO}} = 0;\ \frac{dTSTC_{SO}}{dN_e} = 0. \tag{52}$$

$$\frac{d^2TSTC_{SO}}{dt_{s,SO}{}^2} > 0;\ \frac{d^2TSTC_{SO}}{dt_{s,SO}{}^2} > 0; \tag{53}$$

$$\frac{d^2TSTC_{SO}}{dt_{s,SO}{}^2} \cdot \frac{d^2TSTC_{SO}}{dN_e{}^2} - \left(\frac{d^2TSTC_{SO}}{dN_e dt_{s,SO}}\right)^2 > 0. \tag{54}$$

Based on Eq. (52), we have:

$$t_{s,SO} = t^* - \frac{2\lambda\tau}{(\lambda+\beta)(s^2-\tau^2)}N - \frac{\gamma}{(\beta+\gamma)(s+\tau)}N; \tag{55}$$

$$N_e = \frac{N\gamma}{\beta+\gamma}. \tag{56}$$

For Eq. (53), we have $\frac{d^2TSTC_{SO}}{dt_{s,SO}{}^2} = (\beta + \lambda)\frac{1}{2\tau} \cdot (s^2 - \tau^2)$, $\frac{d^2TSTC_{SO}}{dN_e{}^2} = \frac{\beta}{2\tau} + \frac{\gamma}{s+\tau} + \lambda \cdot \left(\frac{s-\tau}{s+\tau}\right)\frac{1}{2\tau}$, which is positive given that $s > \tau$. For (54), based on Eq. (51), we have $\frac{d^2TSTC_{SO}}{dt_{s,SO}{}^2} \cdot \frac{d^2TSTC_{SO}}{dN_e{}^2} - \left(\frac{d^2TSTC_{SO}}{dN_e dt_{s,SO}}\right)^2 = (\beta + \gamma)(\beta + \lambda)\frac{s-\tau}{2\tau}$, which is also positive when $s > \tau$. Hence, the relationship described in Eqs. (53) and (54) always holds, which implies that the values of $t_{s,SO}$ and N_e in Eqs. (55) and (56) support the SO traffic pattern. The rest parameters listed in Proposition 3.1. can then be easily derived. We omit the calculation process here.

Note that in the proof, the feasible region has included all the possible combinations of $(t_{s,SO}, N_e)$. This includes two extreme cases: (i) $t_{s,SO} = t^* - \frac{N_e}{s+\tau}$, where we have a constant departure rate $f_{e,1} = s + \tau$ for early arrivals; (ii) $t_{s,SO} = t^* - \frac{N_e}{s-\tau}$, where we have a constant departure rate $f_{e,2} = s - \tau$ for early arrivals. After solving Eqs. (52) to (54), we find that the value of the derived $t_{s,SO}$ is between $\left(t^* - \frac{N_e}{s-\tau}\right)$ and $\left(t^* - \frac{N_e}{s+\tau}\right)$ at SO. This means that for early arrival, the SO traffic pattern matches neither of the above-mentioned two cases. The only exception is that when $\tau = 0$, we have $f_{e,1} = f_{e,2} = s$. This completes the proof. □

B.3 Proof. Proposition 4.1.

By checking the second-order derivative of $TSTC_{UE,1}$, we have $\frac{d^2 TSTC_{UE,1}}{d\tau^2} = \frac{\beta N^2}{(\beta+\gamma)}\left(\frac{4\lambda\tau(3s^2+\tau^2)}{(s^2-\tau^2)^3} + \frac{2\gamma}{(s+\tau)^3}\right) > 0$, which means that $TSTC_{UE,1}$ is convex with regards to τ. When τ approaches the lower bound, i.e. $\tau \to 0$, we have $\frac{dTSTC_{UE,1}}{d\tau} = \frac{\beta N^2}{(\beta+\gamma)s^2}(2\lambda - \gamma)$; when τ approaches the upper bound, i.e. $\tau \to s$, we have $\frac{dTSTC_{UE,1}}{d\tau} \to +\infty$. It implies that if $\lambda \geq \frac{\gamma}{2}$, the relationship $\frac{dTSTC_{UE,1}}{d\tau} > 0$ always holds over the domain $\tau \in [0, s]$, under which circumstance we should let $\tau \to 0$ to achieve the minimum $TSTC_{UE,1}$. On the other hand, if $\lambda < \frac{\gamma}{2}$, we have: (i) $\frac{dTSTC_{UE}}{d\tau} < 0$ within the domain $\tau \in [0, s \cdot \frac{\gamma - 2\sqrt{\lambda(\gamma-\lambda)}}{\gamma-2\lambda})$; (ii) $\frac{dTSTC_{UE}}{d\tau} = 0$ at the point $\tau' = s \cdot \frac{\gamma - 2\sqrt{\lambda(\gamma-\lambda)}}{\gamma-2\lambda}$; (iii) $\frac{dTSTC_{UE}}{d\tau} > 0$ within the domain $\tau \in (s \cdot \frac{\gamma - 2\sqrt{\lambda(\gamma-\lambda)}}{\gamma-2\lambda}, s]$. Under this circumstance, we should let $\tau \to \tau' = s \cdot \frac{\gamma - 2\sqrt{\lambda(\gamma-\lambda)}}{\gamma-2\lambda}$ to minimise the $TSTC_{UE,1}$. This completes the proof. □

B.4 Proof. Proposition 4.2.

By taking the first-order and the second-order derivatives of $TSTC_{SO}$ with respect to τ, we have:

$$\frac{dTSTC_{SO}}{d\tau} = \beta \cdot \left[0.5 \cdot \frac{\lambda^2}{(\lambda+\beta)^2} N^2 \left(\frac{1}{s-\tau}\right)^2 - 0.5 \cdot \frac{(\gamma-\lambda)\beta}{(\lambda+\beta)(\beta+\gamma)} \left(\frac{\lambda}{\lambda+\beta} + \frac{\gamma}{\beta+\gamma}\right) N^2 \left(\frac{1}{s+\tau}\right)^2\right] - \gamma \cdot \left[0.5 \cdot \left(\frac{\beta}{\beta+\gamma}\right)^2 N^2 \left(\frac{1}{s+\tau}\right)^2\right] + \lambda \cdot \left[0.5 \cdot \left(\frac{\beta}{\lambda+\beta}\right)^2 \left(\left(\frac{1}{s-\tau}\right)^2 + \left(\frac{1}{s+\tau}\right)^2\right) N^2\right]; \quad (57)$$

$$\frac{d^2TSTC_{SO}}{d\tau^2} = \beta \cdot \left[\frac{\lambda^2}{(\lambda+\beta)^2} N^2 \left(\frac{1}{s-\tau}\right)^3 + \frac{(\gamma-\lambda)\beta}{(\lambda+\beta)(\beta+\gamma)} \left(\frac{\lambda}{\lambda+\beta} + \frac{\gamma}{\beta+\gamma}\right) N^2 \left(\frac{1}{s+\tau}\right)^3\right] + \gamma \cdot \left[\left(\frac{\beta}{\beta+\gamma}\right)^2 N^2 \left(\frac{1}{s+\tau}\right)^3\right] + \lambda \cdot \left[\left(\frac{\beta}{\lambda+\beta}\right)^2 \left(\left(\frac{1}{s-\tau}\right)^3 - \left(\frac{1}{s+\tau}\right)^3\right) N^2\right]. \quad (58)$$

Given that $\frac{d^2TSTC_{SO}}{d\tau^2} > 0$ over the feasible region $\tau \in [0, s)$, $TSTC_{SO}(\tau)$ is strictly convex. To minimise the value of $TSTC_{SO}$, we let $\frac{dTSTC_{SO}}{d\tau} = 0$, and have:

$$\beta \cdot \left[0.5 \cdot \frac{\lambda^2}{(\lambda+\beta)^2} N^2 \left(\frac{1}{s-\tau}\right)^2 - 0.5 \cdot \frac{(\gamma-\lambda)\beta}{(\lambda+\beta)(\beta+\gamma)} \left(\frac{\lambda}{\lambda+\beta} + \frac{\gamma}{\beta+\gamma}\right) N^2 \left(\frac{1}{s+\tau}\right)^2\right] - \gamma \cdot \left[0.5 \cdot \left(\frac{\beta}{\beta+\gamma}\right)^2 N^2 \left(\frac{1}{s+\tau}\right)^2\right] + \lambda \cdot \left[0.5 \cdot \left(\frac{\beta}{\lambda+\beta}\right)^2 \left(\left(\frac{1}{s-\tau}\right)^2 + \left(\frac{1}{s+\tau}\right)^2\right) N^2\right] = 0. \quad (59)$$

By simplifying Eq. (59), we can get:

$$[\lambda(\beta+\gamma)](s+\tau)^2 = [(\gamma-\lambda)\beta](s-\tau)^2. \quad (60)$$

To obtain the optimal solution τ, we solve Eq. (60), and have:

(i) If $\lambda(\beta+\gamma) > [(\gamma-\lambda)\beta]$, i.e. $\lambda > \frac{\gamma\beta}{2\beta+\gamma}$, there exists no real number solution. To minimise $TSTC_{SO}$, τ should approach nil due to the strict convexity of $TSTC_{SO}$;

(ii) If $\lambda(\beta+\gamma) = [(\gamma-\lambda)\beta]$, i.e. $\lambda = \frac{\gamma\beta}{2\beta+\gamma}$, the optimal solution under the SO condition is $\tau_{SO} = 0$;

(iii) If $\lambda(\beta+\gamma) < [(\gamma-\lambda)\beta]$, i.e. $0 < \lambda < \frac{\gamma\beta}{2\beta+\gamma}$, the optimal solution under the SO condition is $\tau_{SO} = s \cdot \left(\sqrt{\frac{(\gamma-\lambda)\beta}{\lambda(\beta+\gamma)}} - 1\right) / \left(\sqrt{\frac{(\gamma-\lambda)\beta}{\lambda(\beta+\gamma)}} + 1\right)$.

This completes the proof. □

Appendix C. Regimes

C.1 Regime z_1

To achieve the system-optimum traffic pattern as discussed in Section 3, we propose the time-varying tolling scheme (regime z_1). We denote the tolling fee for departure time from home t, i.e. the arrival time to the inbound bottleneck, as $\rho(t)$. We assume that commuters always choose the parking space as close to the workplace as possible to reduce the individual travel disutility, i.e. earlier departure implies closer parking. Then, the following time-varying tolling scheme can be derived to support the SO in AV morning commute under capacity allocation:

$$\rho(t)=\begin{cases}\rho\left(t_{s,SO}\right), & t\in[0,t_{s,SO}]\\ \rho\left(t_{s,SO}\right)+\left(t-t_{s,SO}\right)\left(\beta-\dfrac{\lambda w(s-\tau)}{m}\right), & t\in(t_{s,SO},\bar{t}]\\ \rho(\bar{t})+(t-\bar{t})\left(\beta-\dfrac{\lambda w(s+\tau)}{m}-\dfrac{2\lambda\tau}{s-\tau}\right), & t\in(\bar{t},t^*]\\ \rho(t^*)+(t-t^*)\left(-\gamma-\dfrac{\lambda w(s+\tau)}{m}-\dfrac{2\lambda\tau}{s-\tau}\right), & t\in(t^*,t_{e,SO}]\\ \rho\left(t_{e,SO}\right), & t\in(t_{e,SO},+\infty)\end{cases} \tag{61}$$

where we have $\rho\left(t_{s,SO}\right)=\rho_0+\frac{\lambda wN}{m}$, $\rho(\bar{t})=\rho_0+\frac{\lambda\beta}{(\beta+\lambda)}\frac{N}{(s-\tau)}+\frac{\beta}{(\beta+\lambda)}\frac{\lambda wN}{m}$, $\rho(t^*)=\rho_0+\frac{\beta\gamma}{(\beta+\gamma)}\frac{N}{(s+\tau)}+\frac{2\lambda\beta}{(\beta+\gamma)}\frac{\tau N}{(s^2-\tau^2)}+\frac{\beta}{(\beta+\gamma)}\frac{\lambda wN}{m}$, $\rho\left(t_{e,SO}\right)=\rho_0$. ρ_0 is a constant which represents the tolling fee for the commuters arriving at the inbound bottleneck at time $t_{e,SO}$ or later. We omit the derivation process to save space.

With the above tolling scheme, the AV commute pattern under UE conditions can be formed in the SO manner, wherein the generalised travel disutility consists of the travel time cost $c(t,x)$ as formulated in Eq. (1) and the tolling fee. Under this circumstance, no one can further reduce the individual generalised travel disutility by unilaterally changing the departure time and/or parking location. By comparing $\rho\left(t_{s,SO}\right)$ and $\rho\left(t_{e,SO}\right)$, we find that $\rho\left(t_{e,SO}\right)=\rho\left(t_{s,SO}\right)-\frac{\lambda wN}{m}$. This is because, at SO, the first commuter's schedule delay cost is larger than the last commuter's schedule delay cost, while the difference is exactly equal to the last commuter's cost of queuing delay at the outbound bottleneck (please refer to Section 3). Hence, the difference in the travel disutility without the tolling fee between the first and the last commuters is that in the cost of AV self-driving for parking under the free-flow condition, which is $\frac{\lambda wN}{m}$ and equals $\rho\left(t_{s,SO}\right)-\rho\left(t_{e,SO}\right)$. This compensates the last commuter for a disadvantageous parking location due to late departure, with regards to the first commuter.

When looking into the formulations of $\rho(t)$ for the domains $t \in (t_{s,SO}, \bar{t}]$, $t \in (\bar{t}, t^*]$, and $t \in (t^*, t_{e,SO}]$, we find that the gradient with respect to t is the opposite of the marginal in the increase of travel time costs. In this way, the travel time cost and the tolling fee can be balanced, so that at UE with tolls, all the commuters have the identical generalised travel disutility regardless of departure/arrival time. For $t \in (t_{s,SO}, \bar{t}]$, the gradient $\left(\beta - \frac{\lambda w(s-\tau)}{m}\right)$ is positive, as we have the assumption $\beta - \frac{\lambda w(s-\tau)}{m} > 0$ as discussed earlier. For $t \in (\bar{t}, t^*]$, the gradient $\left(\beta - \frac{\lambda w(s+\tau)}{m} - \frac{2\lambda\tau}{s-\tau}\right)$ can be either positive, zero, or negative. When it is positive, the no-toll UE traffic pattern corresponds to Scenario 1 as discussed in Section 2.2; when it is zero or negative, that pattern corresponds to Scenario 2 in Section 2.3. For $t \in (t^*, t_{e,SO}]$, the gradient $\left(-\gamma - \frac{\lambda w(s+\tau)}{m} - \frac{2\lambda\tau}{s-\tau}\right)$ is negative. This is explained as follows. After the official work time t^*, postponing the departure time will increase the schedule delay cost for late arrival penalty, the cruising-for-parking cost under free flow condition and the queuing delay cost at the outbound bottleneck under the SO conditions, while the marginal increases of those costs are respectively γ, $\frac{\lambda w(s+\tau)}{m}$ and $\frac{2\lambda\tau}{s-\tau}$ (please refer to Figure 4). Hence, we reduce the tolling fee for late arrival commuters, so that they are not incentivised to compete for less schedule delay, closer parking, and less queuing delay during AV self-driving, which leads the UE traffic pattern with tolls to the SO form.

C.2 Regime z_2

As an alternative to the tolling strategy, we can impose a parking pricing scheme (regime z_2), in order to achieve the system optimum. In real-world practice, the location-dependent parking fee $p(x)$ is more widely adopted than tolling, given that charging parking fee requires lower operation costs, and in most cases, does not impede traffic flow. Under the assumption that earlier departure corresponds to closer parking, we denote $x_{s,SO}$, $\bar{\bar{x}}$, x^*, and $x_{e,SO}$ as the parking locations for commuters departing from home at $t_{s,SO}$, $\bar{t}$, t^* and $t_{e,SO}$, respectively. We then have $x_{s,SO} = x_0$, $\bar{x} = x_0 + \frac{\lambda}{\beta+\lambda}\frac{N}{m}$, $x^* = x_0 + \frac{\gamma}{\beta+\gamma}\frac{N}{m}$, $x_{e,SO} = x_0 + \frac{N}{m}$. Without loss of generality, we let $p(x_{e,SO}) = p_0$, $p_0 \geq 0$, and derive the parking pricing strategy as follows:

$$p(x) = \begin{cases} p(x_{s,SO}) + \left(\frac{(x - x_{s,SO})m}{s-\tau}\right)\left(\beta - \frac{\lambda w(s-\tau)}{m}\right), & x \in [x_{s,SO}, \bar{x}] \\ p(\bar{x}) + \left(\frac{(x-\bar{x})m}{s+\tau}\right)\left(\beta - \frac{\lambda w(s+\tau)}{m} - \frac{2\lambda\tau}{s-\tau}\right), & x \in (\bar{x}, x^*] \\ p(x^*) + \left(\frac{(x-x^*)m}{s+\tau}\right)\left(-\gamma - \frac{\lambda w(s+\tau)}{m} - \frac{2\lambda\tau}{s-\tau}\right), & x \in (x^*, x_{e,SO}] \\ p(x_{e,SO}), & x \in (x_{e,SO}, +\infty) \end{cases} \quad (62)$$

where $p(x_{s,SO}) = p_0 + \frac{\lambda wN}{m}$, $p(\bar{x}) = p_0 + \frac{\lambda\beta}{(\beta+\lambda)}\frac{N}{(s-\tau)} + \frac{\beta}{(\beta+\lambda)}\frac{\lambda wN}{m}$, $p(x^*) = p_0 + \frac{\beta\gamma}{(\beta+\gamma)}\frac{N}{(s+\tau)} + \frac{2\lambda\beta}{(\beta+\gamma)}\frac{\tau N}{(s^2-\tau^2)} + \frac{\beta}{(\beta+\gamma)}\frac{\lambda wN}{m}$, $p(x_{e,SO}) = p_0$. It can be verified that the user-equilibrium traffic pattern with the parking fee $p(x)$ satisfies the SO conditions for AV commutes under capacity allocation, and we omit the proofs here to save space.

References

Arnott, R., De Palma, A., & Lindsey, R. (1991). A temporal and spatial equilibrium analysis of commuter parking. *Journal of Public Economics*, *45*(3), 301-335.

Arnott, R., De Palma, A., & Lindsey, R. (1993). A structural model of peak-period congestion: A traffic bottleneck with elastic demand. *The American Economic Review*, 161-179.

Arnott, R., & Inci, E. (2006). An integrated model of downtown parking and traffic congestion. *Journal of Urban Economics*, *60*(3), 418-442.

Burns, L. D. (2013). A vision of our transport future. *Nature*, *497*(7448), 181-182.

Chen, Z., Yin, Y., He, F., & Lin, J.L. (2015). Parking reservation for managing downtown curbside parking. *Transportation Research Record: Journal of the Transportation Research Board*, (2498), 12-18.

Di, Z., & Yang, L. (2020). Reversible lane network design for maximizing the coupling measure between demand structure and network structure. *Transportation Research Part E: Logistics and Transportation Review*, *141*, 102021.

Duell, M., Levin, M. W., Boyles, S. D., & Waller, S. T. (2016). Impact of autonomous vehicles on traffic management: Case of dynamic lane reversal. *Transportation Research Record*, *2567*(1), 87-94.

Fosgerau, M. (2011). How a fast lane may replace a congestion toll. *Transportation Research Part B: Methodological*, *45*(6), 845-851.

Hausknecht, M., Au, T. C., Stone, P., Fajardo, D., & Waller, T. (2011, October). Dynamic lane reversal in traffic management. In *2011 14th International IEEE Conference on Intelligent Transportation Systems (ITSC)* (pp. 1929-1934). IEEE.

He, F., Yin, Y., Chen, Z., & Zhou, J. (2015). Pricing of parking games with atomic players. *Transportation Research Part B: Methodological*, *73*, 1-12.

Inci, E., & Lindsey, R. (2015). Garage and curbside parking competition with search congestion. *Regional Science and Urban Economics*, *54*, 49-59.

Kuwahara, M. (1990). Equilibrium queueing patterns at a two-tandem bottleneck during the morning peak. *Transportation Science*, *24*(3), 217-229.

Levin, M. W., & Boyles, S. D. (2015). Effects of autonomous vehicle ownership on trip, mode, and route choice. *Transportation Research Record*, *2493*(1), 29-38.

Levin, M. W., & Boyles, S. D. (2016). A cell transmission model for dynamic lane reversal with autonomous vehicles. *Transportation Research Part C: Emerging Technologies*, *68*, 126-143.

Levin, M.W., Smith, H., & Boyles, S.D. (2019). Dynamic four-step planning model of empty repositioning trips for personal autonomous vehicles. *Journal of Transportation Engineering, Part A: Systems*, *145*(5), 04019015.

Levin, M.W., Wong, E., Nault-Maurer, B., & Khani, A. (2020). Parking infrastructure design for repositioning autonomous vehicles. *Transportation Research Part C: Emerging Technologies*, *120*, 102838.

Li, Z.C., Huang, H. J., & Yang, H. (2020). Fifty years of the bottleneck model: A bibliometric review and future research directions. *Transportation Research Part B: Methodological*, *139*, 311-342.

Li, Z.C., Lam, W.H., & Wong, S.C. (2012). Modeling intermodal equilibrium for bimodal transportation system design problems in a linear monocentric city. *Transportation Research Part B: Methodological*, *46*(1), 30-49.

Lin, X., Li, M., & He, F. (2018). Nonlinear pricing in linear cities with elastic demands. *Transportation Research Part C: Emerging Technologies*, *95*, 616-635.

Liu, T.L., Huang, H.J., Yang, H., & Zhang, X.N. (2009). Continuum modeling of park-and-ride services in a linear monocentric city with deterministic mode choice. *Transportation Research Part B: Methodological*, *43*(6), 692-707.

Liu, W. (2018). An equilibrium analysis of commuter parking in the era of autonomous vehicles. *Transportation Research Part C: Emerging Technologies*, *92*, 191-207.

Liu, W., & Geroliminis, N. (2016). Modeling the morning commute for urban networks with cruising-for-parking: An MFD approach. *Transportation Research Part B: Methodological*, *93*, 470-494.

Liu, W., & Geroliminis, N. (2017). Doubly dynamics for multi-modal networks with park-and-ride and adaptive pricing. *Transportation Research Part B: Methodological*, *102*, 162-179.

Liu, W., Yang, H., & Yin, Y. (2014). Expirable parking reservations for managing morning commute with parking space constraints. *Transportation Research Part C: Emerging Technologies*, *44*, 185-201.

Liu, Y., & Li, Y. (2017). Pricing scheme design of ridesharing program in morning commute problem. *Transportation Research Part C: Emerging Technologies*, *79*, 156-177.

Ma, R., & Zhang, H.M. (2017). The morning commute problem with ridesharing and dynamic parking charges. *Transportation Research Part B: Methodological*, *106*, 345-374.

Qian, Z.S., & Rajagopal, R. (2014). Optimal dynamic parking pricing for morning commute considering expected cruising time. *Transportation Research Part C: Emerging Technologies*, *48*, 468-490.

Qian, Z.S., Xiao, F.E., & Zhang, H.M. (2011). The economics of parking provision for the morning commute. *Transportation Research Part A: Policy and Practice*, *45*(9), 861-879.

Qian, Z.S., Xiao, F.E., & Zhang, H.M. (2012). Managing morning commute traffic with parking. *Transportation Research Part B: Methodological*, *46*(7), 894-916.

Soteropoulos, A., Berger, M., & Ciari, F. (2019). Impacts of automated vehicles on travel behaviour and land use: an international review of modelling studies. *Transport Reviews*, *39*(1), 29-49.

Su, Q., & Wang, D. Z. (2020). On the morning commute problem with distant parking options in the era of autonomous vehicles. *Transportation Research Part C: Emerging Technologies*, *120*, 102799.

Tang, Z.Y., Tian, L.J., & Wang, D.Z. (2021). Multi-modal morning commute with endogenous shared autonomous vehicle penetration considering parking space constraint. *Transportation Research Part E: Logistics and Transportation Review*, *151*, 102354.

Tian, L. J., Sheu, J. B., & Huang, H. J. (2019). The morning commute problem with endogenous shared autonomous vehicle penetration and parking space constraint. *Transportation Research Part B: Methodological*, *123*, 258-278.

Vickrey, W. S. (1969). Congestion theory and transport investment. *The American Economic Review*, *59*(2), 251-260.

Wang, H., Meng, Q., Wang, J., & Zhao, D. (2021). An electric-vehicle corridor model in a dense city with applications to charging location and traffic management. *Transportation Research Part B: Methodological*, *149*, 79-99.

Wang, J., Zhang, X., Wang, H., & Zhang, M. (2019). Optimal parking supply in bi-modal transportation network considering transit scale economies. *Transportation Research Part E: Logistics and Transportation Review*, *130*, 207-229.

Wei, B., Zhang, X., Liu, W., Saberi, M., & Waller, S. T. (2022). Capacity allocation and tolling-rewarding schemes for the morning commute with carpooling. *Transportation Research Part C: Emerging Technologies*, *142*, 103789.

Wu, W., Zhang, F., Liu, W., & Lodewijks, G. (2020). Modelling the traffic in a mixed network with autonomous-driving expressways and non-autonomous local streets. *Transportation Research Part E: Logistics and Transportation Review*, *134*, 101855.

Xiao, F., Shen, W., & Zhang, H. M. (2012). The morning commute under flat toll and tactical waiting. *Transportation Research Part B: Methodological*, *46*(10), 1346-1359.

Xiao, L. L., Liu, T. L., & Huang, H. J. (2016). On the morning commute problem with carpooling behavior under parking space constraint. *Transportation Research Part B: Methodological*, *91*, 383-407.

Xiao, L. L., Liu, T. L., Huang, H. J., & Liu, R. (2021). Temporal-spatial allocation of bottleneck capacity for managing morning commute with carpool. *Transportation Research Part B: Methodological*, *143*, 177-200.

Zhang, X., Liu, W., Waller, S. T., & Yin, Y. (2019a). Modelling and managing the integrated morning-evening commuting and parking patterns under the fully autonomous vehicle environment. *Transportation Research Part B: Methodological*, *128*, 380-407.

Zhang, X., Liu, W., & Waller, S. T. (2019b). A network traffic assignment model for autonomous vehicles with parking choices. *Computer-Aided Civil and Infrastructure Engineering*, *34*(12), 1100-1118.

Zhang, X., Robson, E., & Waller, S. T. (2021). An integrated transport and economic equilibrium model for autonomous transportation systems considering parking behavior. *Computer-Aided Civil and Infrastructure Engineering*, *36*(7), 902-921.

Zhang, X.N., Huang, H. J., & Zhang, H.M. (2008). Integrated daily commuting patterns and optimal road tolls and parking fees in a linear city. *Transportation Research Part B: Methodological, 42*(1), 38-56.

Zhang, X.N., Yang, H., & Huang, H.J. (2011). Improving travel efficiency by parking permits distribution and trading. *Transportation Research Part B: Methodological*, *45*(7), 1018-1034.

Zhu, Z., Li, X., Liu, W., & Yang, H. (2019). Day-to-day evolution of departure time choice in stochastic capacity bottleneck models with bounded rationality and various information perceptions. *Transportation Research Part E: Logistics and Transportation Review*, *131*, 168-192.